HELICOPTER GUST RESPONSE INCLUDING UNSTEADY AERODYNAMIC STALL EFFECTS

Russell R. Bergquist

United Aircraft Corporation

Prepared for:

Army Air Mobility Research and Development Laboratory

May 1973

AD

USAAMRDL TECHNICAL REPORT 72-68

HELICOPTER GUST RESPONSE INCLUDING UNSTEADY AERODYNAMIC STALL EFFECTS

By

Russell R. Bergquist

May 1973

EUSTIS DIRECTORATE
U. S. ARMY AIR MOBILITY RESEARCH AND DEVELOPMENT LABORATORY
FORT EUSTIS, VIRGINIA

CONTRACT DAAJ02-71-C-0024
SIKORSKY AIRCRAFT DIVISION
UNITED AIRCRAFT CORPORATION
STRATFORD, CONNECTICUT

Approved for public release;
distribution unlimited.

51

DISCLAIMERS

The findings in this report are not to be construed as an official Department of the Army position unless so designated by other authorized documents.

When Government drawings, specifications, or other data are used for any purpose other than in connection with a definitely related Government procurement operation, the U. S. Government thereby incurs no responsibility nor any obligation whatsoever; and the fact that the Government may have formulated, furnished, or in any way supplied the said drawings, specifications, or other data is not to be regarded by implication or otherwise as in any manner licensing the holder or any other person or corporation, or conveying any rights or permission, to manufacture, use, or sell any patented invention that may in any way be related thereto.

Trade names cited in this report do not constitute an official endorsement or approval of the use of such commercial hardware or software.

DISPOSITION INSTRUCTIONS

Destroy this report when no longer needed. Do not return it to the originator.

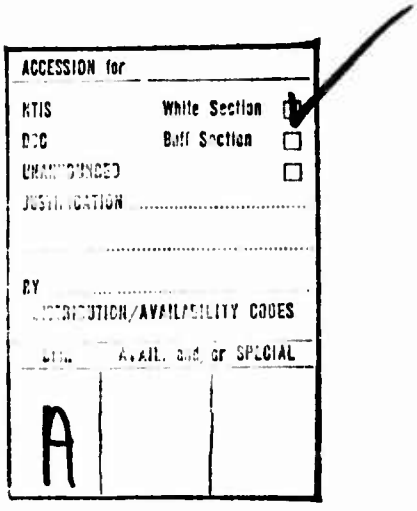

Unclassified
Security Classification

DOCUMENT CONTROL DATA - R & D

(Security classification of title, body of abstract and indexing annotation must be entered when the overall report is classified)

1. ORIGINATING ACTIVITY (Corporate author) Sikorsky Aircraft Division United Aircraft Corporation Stratford, Connecticut	2a. REPORT SECURITY CLASSIFICATION Unclassified 2b. GROUP

3. REPORT TITLE

HELICOPTER GUST RESPONSE INCLUDING UNSTEADY AERODYNAMIC STALL EFFECTS

4. DESCRIPTIVE NOTES (Type of report and inclusive dates)

Final Report

5. AUTHOR(S) (First name, middle initial, last name)

Russell R. Bergquist

6. REPORT DATE	7a. TOTAL NO. OF PAGES	7b. NO. OF REFS
May 1973	~~55~~ 57	10

8a. CONTRACT OR GRANT NO.	9a. ORIGINATOR'S REPORT NUMBER(S)
DAAJ02-71-C-0024 b. PROJECT NO. Task 1F162204AA4301 c. d.	USAAMRDL Technical Report 72-68 9b. OTHER REPORT NO(S) (Any other numbers that may be assigned this report)

10. DISTRIBUTION STATEMENT

Approved for public release; distribution unlimited.

11. SUPPLEMENTARY NOTES	12. SPONSORING MILITARY ACTIVITY
	Eustis Directorate U. S. Army Air Mobility R&D Laboratory Fort Eustis, Virginia

13. ABSTRACT

The Sikorsky/UARL Normal Mode Rotor Aeroelastic Analysis (Computer Program Y-200) was modified to provide the capability of predicting the gust-response characteristics of pure and compound, single-rotor helicopters, including the effects of unsteady aerodynamics on rotor blade stall. The analysis was applied to examine the effects or rotor configuration, flight condition, and gust profile variables on rotor response characteristics. Only the short-term, controls-fixed response was investigated. The results were used to assess the accuracy of the gust-alleviation factor relation given by MIL-S-8698 (ARG) and USAAVLABS Technical Report 69-1 and to provide a basis for developing a more accurate relation, In addition, the impact of the gust on other quantities of interest such as blade vibratory moments and forces was briefly studied. Finally, an assessment of the relative importance of some of the assumptions in the analysis was also made. The results generally confirm earlier results indicating that the gust-alleviation factors given by MIL-S-8698 (ARG) are too conservative and can lead to predicted rotor load factors that can be as much as three times too large at high blade loadings. The inclusion of unsteady aerodynamic stall effects in the present study resulted in higher initial load factors than with steady aerodynamics; however, inclusion of other analytical refinements previously believed to be important (such as fuselage motion) may not be necessary.

DD FORM 1 NOV 68 1473 REPLACES DD FORM 1473, 1 JAN 64, WHICH IS OBSOLETE FOR ARMY USE.

Unclassified
Security Classification

14. KEY WORDS	LINK A		LINK B		LINK C	
	ROLE	WT	ROLE	WT	ROLE	WT
Helicopter Gust Response Rotor Aeroelasticity Unsteady Aerodynamics Helicopter Rotor Blades						

DEPARTMENT OF THE ARMY
U. S. ARMY AIR MOBILITY RESEARCH & DEVELOPMENT LABORATORY
EUSTIS DIRECTORATE
FORT EUSTIS, VIRGINIA 23604

This report has been reviewed by the Eustis Directorate, U. S. Army Air Mobility Research and Development Laboratory and is considered to be technically sound.

The information presented is the result of an analytical investigation into the dynamic and aerodynamic response of variously configured helicopters to three types of gusts. The core of this study involved the modeling of Sikorsky's Normal Modes Aeroelastic Response Analysis computer program to permit analysis of the many cases. A major benefit recognized from the investigation is the acquisition of the cited computer program by the Army for current and future design applications.

The technical monitor for this contract was Mr. William T. Alexander, Jr., Technology Applications Division.

SUMMARY

The Sikorsky/UARL Normal Mode Rotor Aeroelastic Analysis (Computer Program Y-200) was modified to provide the capability of predicting the gust-response characteristics of pure and compound, single-rotor helicopters, including the effects of unsteady aerodynamics on rotor blade stall. The analysis was applied to examine the effects of rotor configuration, flight condition, and gust profile variables on rotor response characteristics. Only the short-term, controls-fixed response was investigated. The results were used to assess the accuracy of the gust-alleviation factor relation given by MIL-S-8698 (ARG) and USAAVLABS Technical Report 69-1 (Reference 2) and to provide a basis for developing a more accurate relation. In addition, the impact of the gust on other quantities of interest such as blade vibratory moments and forces was briefly studied. Finally, an assessment of the relative importance of some of the assumptions in the analysis was also made.

The results generally confirm the results of Reference 2, indicating that the gust-alleviation factors given by MIL-S-8698 (ARG) are too conservative and can lead to predicted rotor load factors that can be as much as three times too large at high blade loadings. The inclusion of unsteady aerodynamic stall effects in the present study resulted in higher initial load factors than with steady aerodynamics; however, inclusion of other analytical refinements previously believed to be important (such as fuselage motion) may not be necessary.

FOREWORD

The Sikorsky/UARL Normal Mode Rotor Aeroelastic Analysis (Computer Program Y-200) was modified to provide the capability of predicting the gust-response characteristics of rotary-wing aircraft, including the effects of unsteady aerodynamics on rotor blade stall. The work was sponsored by the Eustis Directorate, U. S. Army Air Mobility Research and Development Laboratory (USAAMRDL) under Contract DAAJ02-71-C-0024, Task 1F162204AA4301.

In addition to the author of this report, principal Sikorsky personnel associated with the project were Messrs. P. Arcidiacono, R. Carlson, G. Thomas, and T. Beddoes. Mr. W. Alexander was the technical representative for USAAMRDL.

TABLE OF CONTENTS

LIST OF ILLUSTRATIONS

LIST OF TABLES

LIST OF SYMBOLS

A_g	gust-alleviation factor (see Equation (4))
a	lift curve slope
b	number of blades
c	blade chord, ft
C_Z	vertical force coefficient, $Z/\pi\rho\Omega^2R^4$
I_B	blade mass moment of inertia about flapping hinge, slug-ft^2
R	blade radius, ft
V	forward velocity, kn or ft/sec
V_G	maximum vertical velocity of gust, positive up, ft/sec
Z	vertical force, positive up, lb
α	angle between shaft and relative wind, positive when top of shaft is tilted aft, rad
γ	blade Lock number, $\rho acr^4/I_B$
$\Delta n_{r,c}$	incremental rotor load factor as determined by the more complete computerized analysis
$\Delta n_{r,s}$	incremental load factor, as determined by the simple, linear analysis (see Equation (3))
λ	inflow ratio, $(V\sin\alpha - \nu)/\Omega R$
μ	advance ratio, $V\cos\alpha/\Omega R$
ν	rotor induced velocity, positive up, ft/sec
ρ	air density, slugs/ft^3
σ	rotor solidity, $bc/\pi R$
Ω	rotor angular rotational velocity, rad/sec

INTRODUCTION

Current procedures for predicting helicopter gust-induced loads involve computing rotor loads by means of a simplified linear theory and modifying these loads by a gust-alleviation factor defined in MIL-S-8698 (ARG). The alleviation factor is shown in Figure 1 and is a function of rotor disc loading alone. Further, no alleviation is allowed for disc loadings greater than 6.0 - a value exceeded by many modern helicopters. Attempts to verify the accuracy of this approach through flight test have been complicated by uncertainties regarding the gust profiles. This has led to side-by-side flight tests of fixed- and rotary-wing aircraft (Reference 1) in order to build a semiempirical bridge between the relatively straightforward fixed-wing stiuation and the more complex situation associated with rotary wings. Limited qualitative results on aircraft of comparable gross weight indicated that the helicopter was less gust sensitive than the fixed-wing aircraft, but extensive quantitative data from this type of test are, obviously, expensive and difficult to obtain. Analytical confirmation of the MIL-S-8698 (ARG) gust-alleviation factor has been hampered by the lack of an analysis which can handle both the transient response of the helicopter and the aeroelastic response of the rotor blades, while, simultaneously, providing a reasonably complete modeling of the rotor aerodynamic environment. An improved gust response analysis (described in Reference 2) has indicated that current procedures are too conservative. The primary objectives of this investigation were (1) to develop a similar analysis based on the rotor aeroelastic and unsteady stall aerodynamic techniques developed at Sikorsky Aircraft and the United Aircraft Research Laboratories and (2) to apply the analysis to predict rotor gust-alleviation factors for comparison with those given in MIL-S-8698 (ARG) and in Reference 2. The resulting analysis was programmed for solution on a digital computer. The computer program and its associated users manuals (References 3 and 4) have been provided to the Eustis Directorate. Familiarity with the program and its documentation will provide additional insight into the results presented in this report.

FACTORS INFLUENCING HELICOPTER GUST RESPONSE

The computation of gust-induced loads for helicopters is a difficult analytical task because the rotary-wing lifting system is a complex aeroelastic mechanism operating in complicated aerodynamic environment. Principal factors which can be expected to influence the gust response of a helicopter are described briefly below.

1. Rotor Blade Response. Helicopter rotors differ from fixed wings in that the blades (wings) of the rotor are relatively flexible and in many cases are articulated relative to the fuselage. The blades, therefore, are much more responsive to gust loads than is the aircraft as a whole and react in such a way as to reduce or isolate the impact of the gust on the fuselage. Any factor influencing the flatwise response of the blade is, threfore, potentially important.

2. Fixed-Wing Response. If the helicopter is fitted with fixed wings (compound configuration), additional gust loads are, of course, generated. These can be treated using available fixed-wing techniques and are not of primary concern in this study.

3. Rotor Aerodynamic Modeling. The ability of a rotor to generate a load factor during a gust encounter will depend on the proximity of the blade trim angle of attack to stall. A rotor operating on the verge of stall prior to a gust encounter can be expected to generate less additional lift due to the gust than can a rotor initially operating further away from stall. The modeling of stall aerodynamics is important; therefore, the impact of unsteady aerodynamics on rotor stall was investigated in this study.

4. Gust Characteristics. Gust profile and amplitude are, of course, potentially important factors. In addition, the speed of the helicopter as it penetrates a given gust front can be expected to be a significant factor.

5. Control System Inputs. The ultimate effect of the gust on the helicopter must be influenced by any reaction of the pilot or stability augmentation system to the initial loads produced by the gust. It is possible that the largest loads produced by the gust will not be the initial loads but rather those associated with the longer term response of the coupled system represented by the aircraft, pilot, and stability augmentation system (see Figure 2). These longer term effects depend on the specific design characteristics of the aircraft system and no attempt was made to model them in the present study. Hence, the gust-induced loads considered are the initial loads caused by the gust for a control-fixed rotor operating condition.

DESCRIPTION OF THE ANALYSIS

Complete documentation of the equations used in the analysis is given in Reference 3, while procedures for running the associated computer program may be found in Reference 4.

Briefly, the analysis is essentially a digital flight simulator that can be used to determine the fully coupled rotor/airframe response of a helicopter in free flight. This is accomplished by the numerical integration of the blade/airframe equations of motion on a digital computer. Efforts have been made to provide a modular computer program so that various facets of the analysis may be easily updated as more refined analytical techniques are developed. The principal technical assumptions and features of the analysis are listed below.

1. The blade elastic response is determined using a modal approach based on the equations defined in References 3, 5, and 6.

2. The aerodynamic modeling of the blade includes unsteady aerodynamic effects based on the equations and tabulations defined in Reference 6.

3. Provision is made for specifying a distribution of induced velocities (inflow) over the rotor disc. Such distribution for steady level flight can be computed from analyses available in the literature (Reference 7). Since similar analyses for transient flight are not fully developed, rotor induced velocities were assumed constant in this investigation.

4. The response of each individual blade is considered.

5. The fuselage is a rigid (nonelastic) body having six degrees of freedom. Provisions for fixed wings are included. The aerodynamic forces on the wings are computed using simple, finite-span wing theory, neglecting stall and unsteady effects. Alternatively, the wings can be included with the fuselage aerodynamics and handled as described in assumption 6.

6. Fuselage aerodynamic forces and moments are determined using steady, nonlinear, empirical data loaded into the computer program via punched cards.

SIMPLE LINEAR GUST THEORY

As stated earlier, it was desired to cast the results obtained in this investigation in terms of correction factors (gust-alleviation factors) that could be applied to results obtained from a simple theory. If reasonably consistent factors of this type could be evolved, the need for running an expensive computer program might be eliminated in design analysis and a simple specification eventually evolved.

The simple theory used is that defined in Reference 8, in which blade stall and compressibility effects are neglected. In addition, it is assumed here that the gust is sharp-edged and is instantaneously applied to the entire rotor. The increment in rotor load factor produced by the gust is then given by Equation (1).

$$\Delta n_{r,s} = \frac{\Delta\Sigma}{GW} = \frac{\pi\rho R^2(\Omega R)^2 \frac{\partial(C_Z/\sigma)}{\partial\lambda} \sigma\Delta\lambda_G}{\pi\rho R^2(\Omega R)^2 (C_Z/\sigma)_{1g}\sigma} \qquad (1)$$

or

$$\Delta n_{r,s} = \frac{\partial(C_Z/\sigma)}{\partial\lambda} \frac{1}{(C_Z/\sigma)_{1g}} \Delta\lambda_G \qquad (2)$$

But $\Delta\lambda_G$ is simply $V_G/\Omega R$; hence

$$\Delta n_{r,s} = \frac{\partial(C_Z/\sigma)}{\partial\lambda} \frac{1}{(C_Z/\sigma)_{1g}} \frac{V_G}{\Omega R} \qquad (3)$$

The ratio of the Δn_r computed by the more complete computerized analysis developed under this contract to the value given by Equation (3) represents a gust-alleviation factor which can be used to correct the load factor results given by Equation (3). Thus:

$$A_g = \frac{\Delta n_{r,c}\ (\text{"complete" analysis})}{\Delta n_{r,s}\ (\text{"simple" analysis})} \qquad (4)$$

Hopefully, if A_g shows reasonably consistent trends, it can be used with some confidence to predict rotor load factors for combinations of parameters other than those considered in this study.

SCOPE OF STUDY

The primary function of the previously described analysis is the determination of the helicopter gust response induced by changes in flight conditions and blade physical properties. Nineteen data points (given in Table I) were run as defined in Phase II of this contract.

Gust-load factors, blade bending moments, vibratory hub loads, and rotor control loads were calculated for a range of values for C_Z/σ, Lock number, advance ratio, and blade flatwise and torsional stiffness. The effect of compounding (addition of a wing) was also investigated. The responses associated with three types of vertical gusts were investigated: sine-squared, ramp, and sharp-edged. The sine-squared gust and the ramp gust reached a maximum value of 50 feet per second at a penetration distance of 90 feet. The gust profiles are displayed in Figure 3. Three types of rotor systems were evaluated: articulated, nonarticulated (hingeless), and gimbaled. The basic rotor configuration can be found in Table II. The rotor blade physical properties are also given in Table II. It may be seen from this table that the nonarticulated blade has the same physical properties as the articulated blade, except for the first two inboard segments, and the gimbaled blade is simply two connected nonarticulated blades. The segment mass of the articulated blade was adjusted to obtain a Lock number of seven. Other Lock numbers were obtained by linearly scaling the weight of each segment. In designing the nonarticulated blade, the total blade weight associated with a particular Lock number was held constant by adjusting the weight of the two inboard segments. The torsional inertia was assumed constant for all Lock numbers in order to maintain the same torsional frequencies, since any change in these frequencies would induce an undesired secondary response. The natural frequencies of each of the blades are given in Table III.

The number of modes used varied with the rotor system and advance ratio. For the articulated rotor, three flatwise, two chordwise, and one torsional mode were used. A chordwise-torsional coupling instability was experienced for many of the 0.5 advance ratio nonarticulated *and* gimbaled points. Several check cases were run at stable conditions with and without the torsional degree of freedom. Analysis of these data indicated that only minor effects on the rotor load factor resulted from the suppression of the torsional degree of freedom. For this reason torsion was omitted from the 0.5 advance ratio nonarticulated cases and all of the gimbaled cases.

Because of the sensitivity of the rotor load factor to C_Z/σ, the tolerance of the Z force was held to one percent. This was normally accomplished in three to four iterations. The number of rotor revolutions necessary to establish maximum helicopter and rotor responses during gust penetration varied from two for the high-speed cases to four for the low-speed conditions.

All fuselage and rotor blade physical and aerodynamic properties used in this study have been provided to USAAMRDL as part *of* the computer check case. However, for convenience, the most common fuselage physical properties used are given in Table IV. The fuselage physical and aerodynamic properties were constant for all cases.

ANALYSIS OF RESULTS

EFFECT OF GUST PROFILE

Effect on Incremental Rotor Vertical Force

The effect of gust profile on incremental rotor vertical force was evaluated by the penetration of three gusts with profiles as shown in Figure 3. The helicopter was assumed to penetrate a stationary gust with a velocity of 350 feet per second. This corresponds to an advance ratio of 0.5. An articulated rotor was used.

The first gust evaluated had a sine-squared profile reaching a maximum velocity of 50 feet per second at a penetration distance of 90 feet. The gust velocity then decreased as the sine squared until a penetration distance of 180 feet was attained. At this time the gust velocity was zero and remained zero for all penetration distances greater than 180 feet. The second gust wave form was ramp shaped, with gust velocity increasing linearly with penetration distance from zero at zero distance to a maximum value of 50 feet per second at a penetration distance of 90 feet. The gust velocity remained at 50 feet per second for penetration distances greater than 90 feet. The third gust evaluated was sharp-edged; the value of the gust was assumed to be 50 feet per second, independent of penetration distance.

The time histories of the rotor Z force produced by each gust profile are shown in Figure 5. Of the loads induced by the three gust profiles considered, the load produced by the sharp-edged gust builds up most rapidly and reaches the greatest peak value. The sine-squared and ramp gusts result in similar peak loads at approximately the same time. As the penetration distance increases, however, the loads produced by the sharp-edged gust and the ramp gust tend to merge since their respective terminal velocities are both 50 feet per second, while the value of the sine-squared gust velocity drops back toward zero.

Analysis of the computed results forming the basis for Figure 4 indicates that the maximum rotor vertical force and load factor is reached before the helicopter fuselage has had time to develop any significant gust-induced motion. The vertical velocities of the helicopter associated with the sine-squared, ramp, and sharp-edged gusts are 6 feet per second, 6 feet per second, and 3 feet per second, respectively. These fuselage velocities act to reduce the relative vertical velocity between the aircraft and the gust. The fact that they are relatively small compared to the peak gust velocity of 50 feet per second at the time of maximum load implies that there is little gust alleviation being produced by the fuselage motion.

Effect on Fuselage Vertical Force

A comparison of the fuselage aerodynamic force resulting from encounters with the three gust profiles as previously defined is shown in Figure 4. Very little difference between the ramp gust and the sine-squared gust is noted until the maximum gust velocity has been reached. At this time, as expected, the force generated by the sine-squared gust begins to drop toward

zero while the force generated by the now constant ramp gust drops off slowly as the gust is alleviated by the induced helicopter vertical velocity. The sharp-edged gust causes two sudden jumps in force, the first when the gust reaches the helicopter center of gravity and the second when it reaches the horizontal tail. These discontinuities are the result of the assumption that fuselage and tail forces are defined by steady aerodynamics and that the angles of attack used to compute these forces are those defined by the value of the instantaneous gust velocity at the fuselage c.g. and tail respectively. The fuselage forces are small relative to the rotor forces so that these assumptions are not critical. Thus, the rotor is the predominant element in producing helicopter load factor. It is also the lifting element whose gust characteristics are least amenable to current analyses. The remainder to this report will, therefore, be concerned with the forces generated by the rotor.

Effect on Helicopter Vertical Force

The effect of gust profile on total helicopter response is shown in Figure 5. As expected, the incremental vertical force is approximately equal to the sum of the rotor and fuselage incremental forces. This is not the exact algebraic sum because of the effect of inertia forces due to helicopter acceleration plus the fact that the total force has been resolved from the body axis system into the inertial axis system. As anticipated, the time histories of the helicopter and the rotor forces are quite similar.

Effect on Blade Bending Moment

The effect of gust profile on blade bending moment is generally the same as the effect on vertical forces. The results shown in Figure 6 indicate this to be the case. The sharp-edged gust excites a higher vibratory bending moment with less gust penetration. The sine-squared gust bending response begins to reapproach its steady-state oscillation, while the time histories of the bending moments associated with the sharp-edged and ramp gusts tend to merge with larger vibratory values than that for the steady-state condition. The bending moments displayed in Figure 6 are those calculated at 0.6 radius. This station is the radial position of the maximum vibratory moment in steady flight.

Effect on Torsional Root Bending Moment

The azimuthal variation of root torsional moment during gust penetration for the three types of gusts previously described is shown in Figure 7. The comments made in describing the flatwise bending moment hold here except for a note of the excitation by the sharp-edged gust of the first torsional natural frequency during the first rotor revolution. This is due to stall flutter of the retreating blade produced by high angles of attack. The angle of attack at the 75% radial station reaches 37 degrees as shown in Figure 8, well beyond stall. This plot shows the angle of attack for each of the four blades at 270 deg azimuth angle. Similar excitation of the torsional response is delayed until the second rotor revolution in the case of the sine-squared and ramp gusts. It should be noted that the control load is directly proportional to this moment.

General Discussion of the Effect of Gust Profile

The three types of gust forms evaluated did not produce greatly different peak rotor loads. While the sharp-edged gust did consistently excite somewhat larger maximum responses, it is probably the least realistic of the three profiles. Since other studies, such as Reference 2, have been done using a sine-squared gust, this shape was chosen for use during the rest of this study.

EFFECT OF ROTOR AND FLIGHT CONDITION VARIABLES

Effect of Rotor Loading and Rotor Type on Gust-Alleviation Factor

The variation of the gust-alleviation factor (as computed from Equation (4)) with initial rotor loading is shown in Figure 9 for the three types of rotors analyzed. Rotor loading in this figure has been expressed in terms of both rotor thrust coefficient/solidity ratio and rotor disc loading. It should be noted that disc loading is not a unique function of C_Z/σ but rather depends on the value of density, tip speed, and solidity of the rotor. Values for these quantities are noted on the figure.

The results of Figure 9 indicate that increasing C_Z/σ leads to a large reduction of the gust-alleviation factor. This is similar to the trend noted in Reference 2 and is believed to be related to the loss in average additional lift capability at the higher C_Z/σ's due to the occurrence of stall. The impact of rotor configuration is seen to be of rather secondary importance. Rotor configuration would be expected to influence fuselage motion through the transmittal of differing rotor pitching moments to the airframe, depending on the degree of rotor articulation. The relative insensitivity of the results is believed to be due to the short time required for the initial, controls-fixed load factor to be generated. As a result, the fuselage response to the differing moments is not large and the load factor tends to be dominated by the rotor dynamic response, which is roughly the same for all rotors. This result is also similar to that observed in Reference 2.

Effect of Advance Ratio and Lock Number on Gust-Alleviation Factor

The effect of advance ratio and Lock number on the gust-alleviation factor may be seen in Figure 10. The effects of either parameter are relatively small. The most consistent trend is with blade Lock number, where additional gust alleviation is noted (lower A_G) as Lock number is increased. This alleviation is the result of the lower inertia of the higher Lock number blades which permits a more rapid response of the blade to gust-induced loads. This response reduces the blade angle of attack and, hence, the rotor incremental lift due to the gust.

Effect of Compounding on Gust-Alleviation Factor

The effect of compounding was evaluated by adding wings and reducing rotor lift to 30 percent of the aircraft gross weight. This unloading of the rotor resulted in a greater incremental rotor vertical force since the rotor

was operating further from stall. The effect of compounding may be seen in Figure 11. Both the pure helicopter and the helicopter with wing added had equal gross weights. Therefore, the rotor disc loading was lower for the compound aircraft. As shown in Figure 9, the gust-alleviation factor is larger for lower disc loadings, or the rotor is further from stall for lower loadings. It is this effect that explains the somewhat higher gust-alleviation factors for the compound aircraft.

Effect of Reduced Blade Stiffness on Gust-Alleviation Factor

No significant effects of the gust-alleviation factor were noted when 50 percent reductions in either flatwise or torsional stiffness were made. The primary blade response influencing the rotor load factor is the blade flatwise response (either flapping or bending). Since we are dealing with blades whose flatwise response is dominated by the centrifugal stiffness, it is not surprising that reductions in stiffness have little effect on the blade's dynamic response and, hence, on gust alleviation. This fact is borne out by Figures 12 and 13, which indicate small variations in gust-alleviation factor as the flatwise and torsional stiffnesses are reduced.

Effect of Advance Ratio and Lock Number on Flatwise Stress

The effects of the gust on blade flatwise vibratory stress were examined for several combinations of advance ratio and Lock number. The results are presented in Figure 14 in terms of the ratio of the maximum vibratory stress produced by the gust to the vibratory stress for the trim or steady-state operating condition. The stresses were evaluated at the critical radial stations: at 0.6R for the articulated rotor and at the blade root for the nonarticulated and hingeless rotors. This method of presentation was chosen because of the large variations in trim stresses that can exist between different designs. It is of interest, however, to determine whether a gust encounter causes the stresses to increase by a factor (i.e., stress ratio) which is relatively similar for all rotors, and to determine the degree to which the factor varies with flight condition or other rotor parameters. The results of Figure 14 indicate little variation in stress ratio with either Lock number or advance ratio. Further, the maximum vibratory flatwise stress during the gust encounter may be expected to be about two to four times the steady-state values, depending on the type of rotor configuration. This contrasts with the results of Figure 10 where little difference in gust-alleviation factor was noted for the different configurations. A detailed investigation of the reasons for the observed trends in stress was beyond the scope of this study.

It should also be noted that the ratios shown in Figure 14 are not completely general since they are undoubtedly functions of the gust velocity. Reference 9 indicates that the vibratory stress is approximately linearly related to inflow ratio if large amounts of stall are not present. Thus, dividing the results of Figure 14 by the gust velocity may serve to produce a more generally applicable result. Further investigation is required to substantiate this hypothesis.

Effect of Advance Ratio and Lock Number on Pushrod Load

The effects of the gust on vibratory pushrod load for the articulated rotor are presented in Figure 15. Pushrod loads were not obtained for the non-articulated and gimbaled rotors since a chordwise-torsional coupling instability was experienced for many of the 0.5 advance ratio conditions when the torsional mode was included for these configurations. Pushrod load is calculated by dividing the torsional moment at the blade root by the distance between the pitch axis and the pushrod attachment point. As with flatwise stress in the preceding section, an attempt has been made to generalize the results to some degree by nondimensionalizing by the vibratory pushrod load for the initial trim condition. The results of Figure 15 indicate large variations in pushrod load ratio. The ratio is lower at the 0.5 advance ratio because of the larger vibratory pushrod loads associated with the trim conditions. The results correspond to a specific gust amplitude. Unlike flatwise stress, however, the pushrod loads are less likely to be linear functions of gust velocity but, rather, will probably be more related to the degree of stall present. Thus, the lower pushrod load ratio observed for the 0.5 advance ratio was due primarily to the higher vibratory loads present in the initial trim conditions. At the 0.3 advance ratio the $\gamma = 7$ curve falls below the $\gamma = 10$ curve. It was not apparent from examining the output of these two cases why the crossover occurred. Additional printout would probably be needed to determine the reason. Further work is required to define all important parameters and to produce more generally applicable results.

Effect of Advance Ratio and Lock Number on Rotor Vibratory Force

The effect of the gust on rotor vibrations was briefly examined. Only the vertical force was considered. The results are presented in Figure 16 in terms of a vibratory force ratio. This ratio was obtained by dividing the maximum four-cycle-per-revolution component of the rotor Z force during gust penetration by the steady-state four-cycle-per-revolution value. Although in some flight conditions other frequencies were noted, the four-cycle component was by far the largest (as would be expected for rotors having four blades). For this reason it will be the only frequency discussed. Examination of this figure indicates little or no change in vibratory force ratio with Lock number for the 0.5 advance ratio condition. However, a wide variation may be seen for the 0.3 advance ratio. The primary reason for the difference in the vibratory force ratio associated with the two advance ratios is the small amount of steady flight vibration at the low advance ratio. The same comments made in the last section regarding the generality of the control load ratios also apply here. It should also be noted that the results presented are based on the assumption of constant rotor inflow. In reality, the induced velocity along each blade varies both with radius and with time. Such variations could significantly impact vibration levels; however, their introduction was beyond the scope of this study.

SENSITIVITY OF RESULTS TO ASSUMPTIONS

As discussed in an earlier section of this report, many factors could potentially influence rotor gust-response characteristics. To account for all of

these factors leads to a time-consuming, complex, digital analysis. In the following paragraphs, the results of a brief examination of the importance of some of these factors are discussed. Only the articulated rotor at one operating condition is evaluated. Any conclusions drawn from these results must, therefore, be considered preliminary and should be substantiated by further investigation.

Fuselage Motion

The analysis includes the effects of fuselage motion on the rotor blade aerodynamic and dynamic forces. Figure 17 shows rotor vertical force time histories predicted with and without the effects of fuselage motion. It may be seen from this figure that the effect of the fuselage motion has a negligible effect on the rotor vertical force. This might be expected in view of the short elapsed time required for the maximum load factor to be generated. As noted earlier, the vertical velocity of the fuselage is about 6 feet per second at the time of peak rotor load. This reduces the relative vertical gust velocity by only about 10%.

Unsteady Aerodynamics

The effect of unsteady aerodynamics may be seen in Figure 18. Examination of this figure indicates a fairly significant (approximately 25%) increase in incremental vertical force when unsteady aerodynamics are used. This increase is consistent with the results presented in Reference 10, where it is shown that unsteady hysteresis effects lead to a greater lift capability of the rotor. The net result is the prediction of a more gust sensitive rotor when unsteady aerodynamics are employed.

This result is in apparent contradiction to that in Reference 2 where the effect of "unsteady aerodynamics" was found to be small for the sine-squared gust. The reason for this is that the unsteady aerodynamic effects referred to in the investigation reported herein relate to a stall hysteresis effect which enhances maximum blade lift capability. In Reference 2, such unsteady stall effects have been neglected and only approximations to potential flow unsteady aerodynamic effects were considered.

Torsional Degree of Freedom

Because of the difficulty with the chordwise-torsional coupling instability previously mentioned (see Scope of Study section), the nonarticulated rotor cases with 0.5 advance ratio were run without the torsional degree of freedom and with a single chordwise mode. The effect of these changes for the flight condition previously defined are shown in Figure 19. This figure indicates an increase in incremental rotor vertical force when blade torsional deflections are included. Based on these results, the gust alleviation factors computed for the nonarticulated and gimbaled rotors at an advance ratio of 0.5 are probably somewhat higher than those presented. However, this does not alter the conclusions reached in this investigation.

Gust Penetration

The greatest single reason for lengthy computer runs associated with gust penetration is the necessity for computing response time histories for each individual blade. A calculation was performed using a sudden, sharp-edged gust affecting the entire rotor simultaneously. The resulting vertical force calculation indicated a maximum rotor load factor about equal to that predicted by linear theory. This gives rise to the speculation that a time-variant, sudden gust might be a simple and economical way to predict load factors, since gust penetration and individual blade calculation would not be necessary. It should be noted, however, that this would only be applicable to gusts with finite time slope profiles. Further study along these lines appears to be worthwhile.

COMPARISON OF METHODS

Typical rotor load factors predicted by three methods are shown in Figure 20. The method used in calculating the curve defined by MIL-S-8698 (ARG) employs linear aerodynamic theory in the calculation of incremental Z force and assumes that the gust is both constant with time and affects the entire disc instantaneously. This is a simple and convenient way of calculating load factor. However, as previously discussed, this method does not take into account the gust profile, finite time penetration of the gust, and rotor stall effects. These facts have, to some extent, been recognized and the adoption of a gust-alleviation factor for helicopters with disc loadings up to 6 pounds per square foot is permitted. This factor has been shown in Figure 1. If the curve labeled MIL-S-8698 (ARG) in Figure 20 is compared to the curve calculated by the analysis developed for this study (which includes all of the previously menticned effects), it is immediately obvious that the MIL-S-8698 (ARG) is unduly severe. A relation based on steady stall aerodynamic results proposed by the Bell Helicopter Company (Reference 2) is also shown in this figure. It may be seen that this relation yields lower values of rotor load factor at the low values of C_Z/σ. The reason for this cannot be defined precisely at this time. It may be related to the use of steady stall aerodynamics. The circle shown in Figure 20 represents results obtained from the present analysis when steady stall aerodynamics are used. The agreement between this point and the Bell steady aerodynamic results is good.

The results of Figure 20 imply that the gust-alleviation factor allowed by the MIL-S-8698 (ARG) is too high (i.e., too little alleviation). This is substantiated in the summary plots presented in Figure 21, where gust-alleviation factors computed by the Normal Modes Analysis developed in this study are compared with those of the MIL-S-8698 (ARG) for three types of rotor systems. The conservatism of the MIL-S-8698 (ARG) is particularly evident at the high thrust coefficients where rotor stall becomes a factor limiting the thrust generating capability. The normal modes gust-alleviation factor shown in Figure 21 was calculated at $\mu = .3$ and $\gamma = 10$, except for the $C_Z/\sigma = .04$ condition (where the μ was 0.5). At a $C_Z/\sigma = 0.06$, the variation in gust-alleviation factor due to blade Lock number and stiffness changes is shown. The range is relatively small, and as may be seen from Figures 10 and 12, Lock number is the primary cause of the variation; and the higher

Lock numbers are associated with the lower gust-alleviation factors. The variations shown at $C_Z/\sigma = 0.06$ are believed to be representative of those at other C_Z/σ values; however, further study is required to verify this contention.

CONCLUSIONS

The following conclusions were reached as a result of this study. It should be noted that these are based on the computation of rotor gust-alleviation factors associated with the initial peak load factors produced by various rotor systems mounted on a single fuselage and operating with the controls fixed throughout the gust encounters.

1. The results of this study generally confirm those of Reference 2, indicating that the current method for computing gust-alleviation factors for helicopter rotors (MIL-S-8698 (ARG)) results in unrealistically high values and should be revised.

2. If the gust amplitude is sufficient to cause retreating blade angles of attack greater than the two-dimensional, steady-state stall angle, the inclusion of unsteady aerodynamic effects based on the model of Reference 6 results in gust-alleviation factors which are higher than those based on a steady aerodynamic model such as that used in Reference 2.

3. Principal parameters influencing the gust-alleviation factor appear to be nondimensional blade loading, proximity of the rotor trim point to blade stall, rate of penetration of the rotor into the gust, and blade Lock number. Rotor advance ratio and rotor system type generally had a smaller effect.

RECOMMENDATIONS

1. Experimental studies should be conducted to confirm the analytical results obtained in this investigation.

2. The results of this study should be extended to evaluate longer term gust response effects, including aircraft, pilot, and stability augmentation system variables.

3. A method for modeling the velocities induced over the rotor disc by the rotor wake should be developed for transient operating conditions.

4. There appears to be considerable potential for developing a relatively simpler, yet more accurate, method for predicting gust-induced loads than that now provided by MIL-S-8698 (ARG). The analysis developed in this investigation provides an ideal model against which the validity of various simplifying assumptions can be evaluated. Preliminary results in this study have indicated when possible simplifications might be made (e.g., eliminate fuselage response effects). Further studies should be made to confirm the generality of these initial results and to evolve a revised procedure.

TABLE I. SUMMARY OF DATA POINTS

Case No.	C_Z/σ	μ	γ
	Standard Blade		
1	0.06	0.3	10.0
2	0.06	0.3	13.0
3	0.06	0.3	7.0
4	0.09	0.2	10.0
5	0.06	0.4	10.0
6	0.06	0.5	7.0
7	0.06	0.5	10.0
8	0.06	0.5	13.0
9	0.08	0.3	10.0
10	0.10	0.3	10.0
11	0.04	0.5	10.0
	Torsional Stiffness Reduced 50%		
12	0.06	0.3	10.0
13	0.06	0.5	10.0

TABLE I - Concluded

Case No.	C_Z/σ	μ	γ
	Flatwise Stiffness Reduced 50%		
14	0.06	0.3	10.0
15	0.06	0.5	10.0
	Addition of Wing		
16	0.06	0.3	10.0
17	0.06	0.5	10.0
	Ramp Gust		
18	0.06	0.5	10.0
	Sharp-Edged Gust		
19	0.06	0.5	10.0

TABLE II. BLADE AND ROTOR STANDARD PHYSICAL PROPERTIES

Flight condition	sea level standard
Airfoil	0012
Tip speed, ft/sec	700
Radius, ft	25
No. of blades	4
Blade chord, ft	1.67
Twist, (linear) deg	-8.0
Young's Modulus, psi	10^7

Seg. Length/Radius	Mass, slugs γ=13.0	γ=10.0	γ=7.0	I Flatwise, in^4	I Chordwise, in^4	GJ/10^7 lb-in^2
Articulated Blade						
0.0534	0.797	1.036	1.480	79.00	79.00	61.60
0.0534	0.587	0.751	1.074	79.00	63.00	35.00
0.0534	0.236	0.307	0.439	3.26	36.00	4.45
0.0833	0.367	0.476	0.681	3.18	34.50	4.30
0.0833	0.347	0.451	0.645	3.05	32.80	4.17
0.0833	0.336	0.436	0.623	2.90	31.00	4.00
0.0833	0.323	0.419	0.599	2.80	29.00	3.85
0.0667	0.248	0.322	0.460	2.70	27.30	3.70
0.0667	0.242	0.314	0.449	2.60	26.50	3.60
0.0667	0.237	0.309	0.441	2.50	26.00	3.42
0.0667	0.225	0.292	0.417	2.40	25.00	3.30
0.0500	0.163	0.211	0.302	2.30	24.50	3.15
0.0500	0.159	0.206	0.295	2.20	24.00	3.05
0.0433	0.134	0.174	0.249	2.15	23.50	2.95
0.0565	0.400	0.519	0.741	2.08	23.00	2.85

First station begins at flapping hinge location, e/R = .04.

TABLE II - Concluded

Seg. Length/Radius	Mass, slugs γ=13.0	γ=10.0	γ=7.0	I Flatwise, in^4	I Chordwise, in^4	GJ/10^7 $lb\text{-}in^2$
Nonarticulated and Gimbaled Blade						
0.04	0.287	0.287	0.287	5.00	158.0	61.60
0.1068	1.500	1.500	1.500	60.00	144.0	35.00
0.0534	0.236	0.307	0.439	3.26	115.0	4.45
0.0833	0.367	0.476	0.681	3.18	90.0	4.30
0.0833	0.347	0.451	0.645	3.05	90.0	4.17
0.0833	0.336	0.436	0.623	2.90	90.0	4.00
0.0833	0.323	0.419	0.599	2.80	90.0	3.85
0.0667	0.248	0.322	0.460	2.70	90.0	3.70
0.0667	0.242	0.314	0.449	2.60	90.0	3.60
0.0667	0.237	0.309	0.441	2.50	90.0	3.42
0.0667	0.225	0.292	0.417	2.40	90.0	3.30
0.0500	0.163	0.211	0.302	2.30	90.0	3.15
0.0500	0.159	0.206	0.295	2.20	90.0	3.05
0.0433	0.134	0.174	0.249	2.15	90.0	2.95
0.0565	0.400	0.519	0.741	2.08	90.0	2.85
First station begins at center of rotation.						
Nonarticulated and Gimbaled Blades with Reduced Torsional or Flatwise Stiffness						
Same values as above except that torsion GJ (for reduced torsional stiffness) or flatwise I (for reduced flatwise stiffness) is reduced by 50% at all stations except station one. Station one inertia is unchanged.						

TABLE III. BLADE NATURAL FREQUENCIES
(CYCLES PER REVOLUTION)

	Lock No. γ = 13.0	Lock No. γ = 10.0	Lock No. γ = 7.0
ARTICULATED - STANDARD STIFFNESS			
Rigid Body Flatwise	1.03	1.03	1.03
First Bending Flatwise	2.70	2.66	2.61
Second Bending Flatwise	5.30	5.06	4.81
Third Bending Flatwise	9.13	8.50	7.81
Rigid Body Chordwise	0.25	0.25	0.25
First Bending Chordwise	4.00	3.68	3.33
Second Bending Chordwise	11.40	10.20	8.83
First Bending Torsional	5.72	5.72	5.72

	Lock No. γ = 10.0
ARTICULATED - FLATWISE STIFFNESS REDUCED 50%	
Rigid Body Flatwise	1.03
First Bending Flatwise	2.58
Second Bending Flatwise	4.63
Third Bending Flatwise	7.32

	Lock No. γ = 10.0
ARTICULATED - TORSIONAL STIFFNESS REDUCED 50%	
First Bending Torsional	4.58

TABLE III - Continued

NONARTICULATED - STANDARD STIFFNESS

	Lock No. γ = 13.0	Lock No. γ = 10.0	Lock No. γ = 7.0
First Bending Flatwise	1.12	1.11	1.09
Second Bending Flatwise	2.97	2.87	2.76
Third Bending Flatwise	5.71	5.42	5.10
First Bending Chordwise	1.46	1.30	1.12
Second Bending Chordwise	8.41	7.47	6.39
First Bending Torsional	5.66	5.66	5.66

NONARTICULATED - FLATWISE STIFFNESS REDUCED 50%

	Lock No. γ = 10.0
First Bending Flatwise	1.10
Second Bending Flatwise	2.76
Third Bending Flatwise	4.97

NONARTICULATED - TORSIONAL STIFFNESS REDUCED 50%

	Lock No. γ = 10.0
First Bending Torsional	4.54

GIMBALED - STANDARD STIFFNESS

	Lock No. γ = 13.0	Lock No. γ = 10.0	Lock No. γ = 7.0
Rigid Body Flatwise	1.00	1.00	1.00
First Bending Flatwise	1.12	1.11	1.09
Second Bending Flatwise	2.57	2.54	2.52
Third Bending Flatwise	2.97	2.87	2.76

TABLE III - Concluded

GIMBALED - FLATWISE STIFFNESS REDUCED 50%

	Lock No. $\gamma = 10.0$
Rigid Body Flatwise	1.00
First Bending Flatwise	1.10
Second Bending Flatwise	2.48
Third Bending Flatwise	2.76

For chordwise and torsional frequencies see nonarticulated section.

TABLE IV. FUSELAGE PHYSICAL PROPERTIES	
Fuselage station data reference, in.	300.0
Fuselage station main rotor, in.	300.0
Fuselage station center of gravity, in.	300.0
Fuselage station tail rotor, in.	667.0
Waterline data reference, in.	249.0
Waterline main rotor, in.	294.0
Waterline center of gravity, in.	249.0
Waterline tail rotor, in.	298.5
I_{xx}, slug-ft^2	9500.0
I_{yy}, slug-ft^2	37500.0
I_{zz}, slug-ft^2	34200.0
I_{xz}, slug-ft^2	1500.0

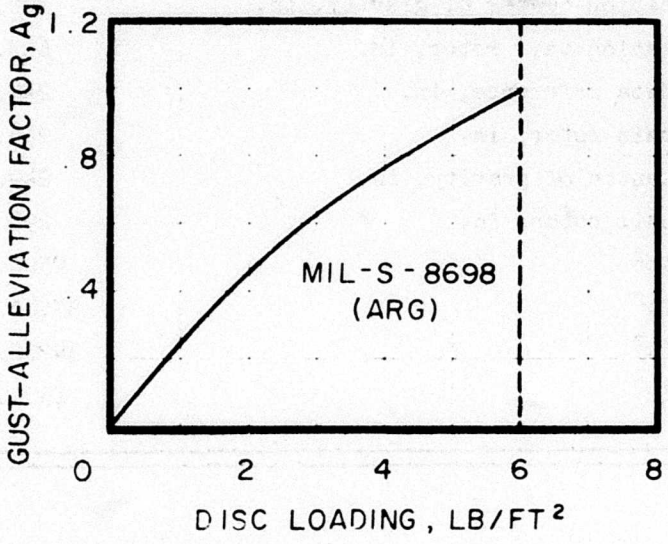

Figure 1. Gust-Alleviation Factor as Allowed by Military Specification.

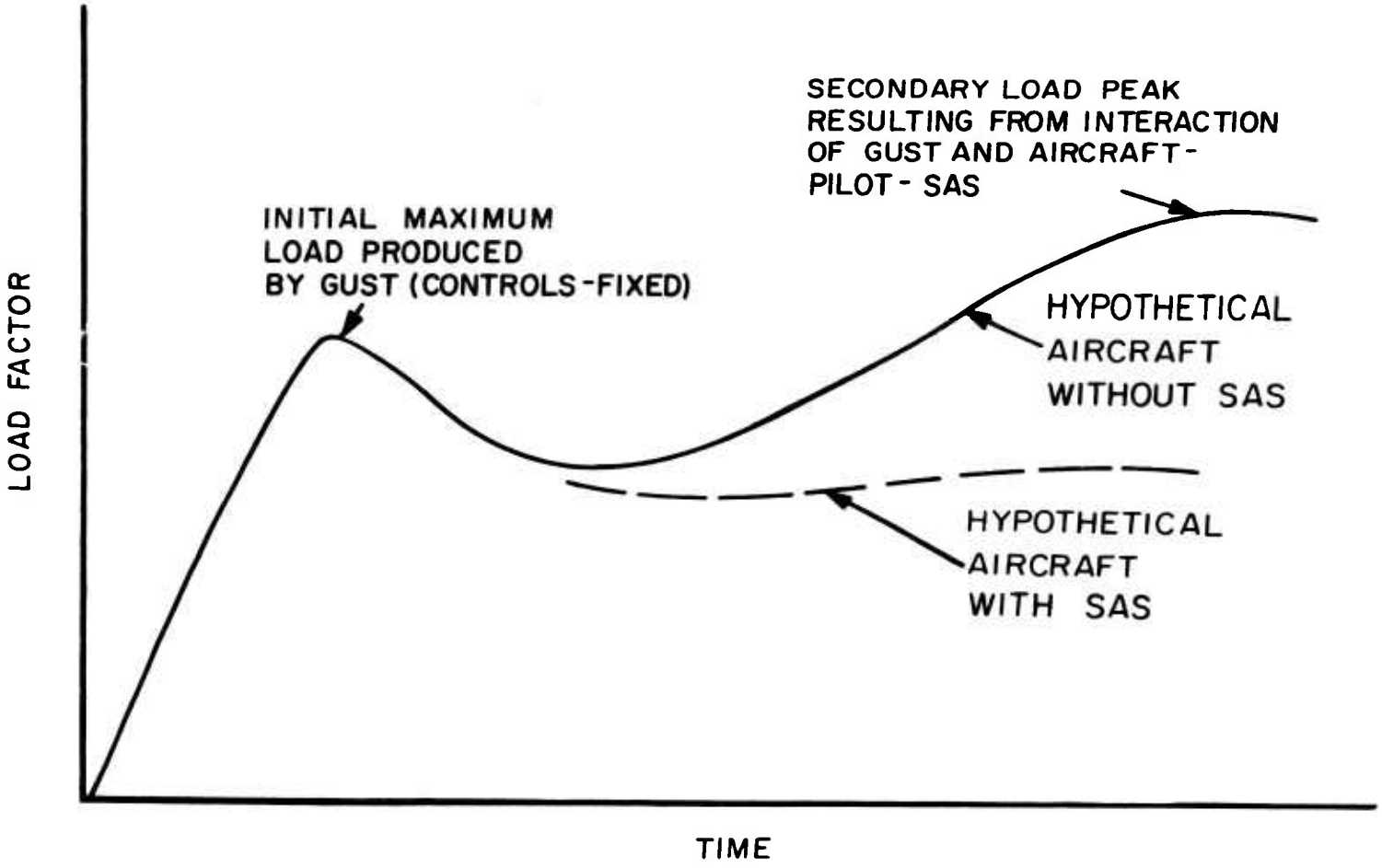

Figure 2. Schematic of Possible Load Factor Time Histories.

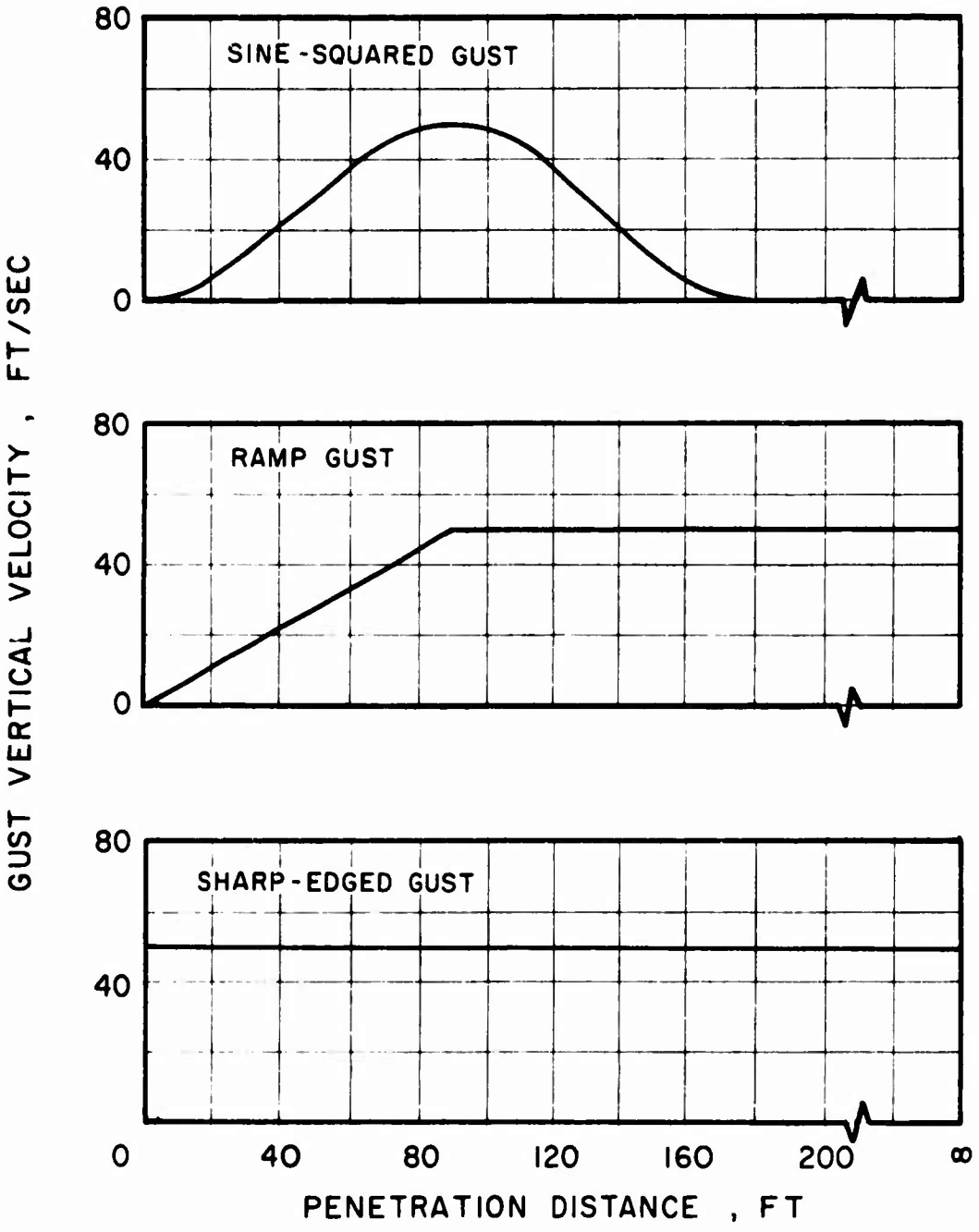

Figure 3. Gust Profiles.

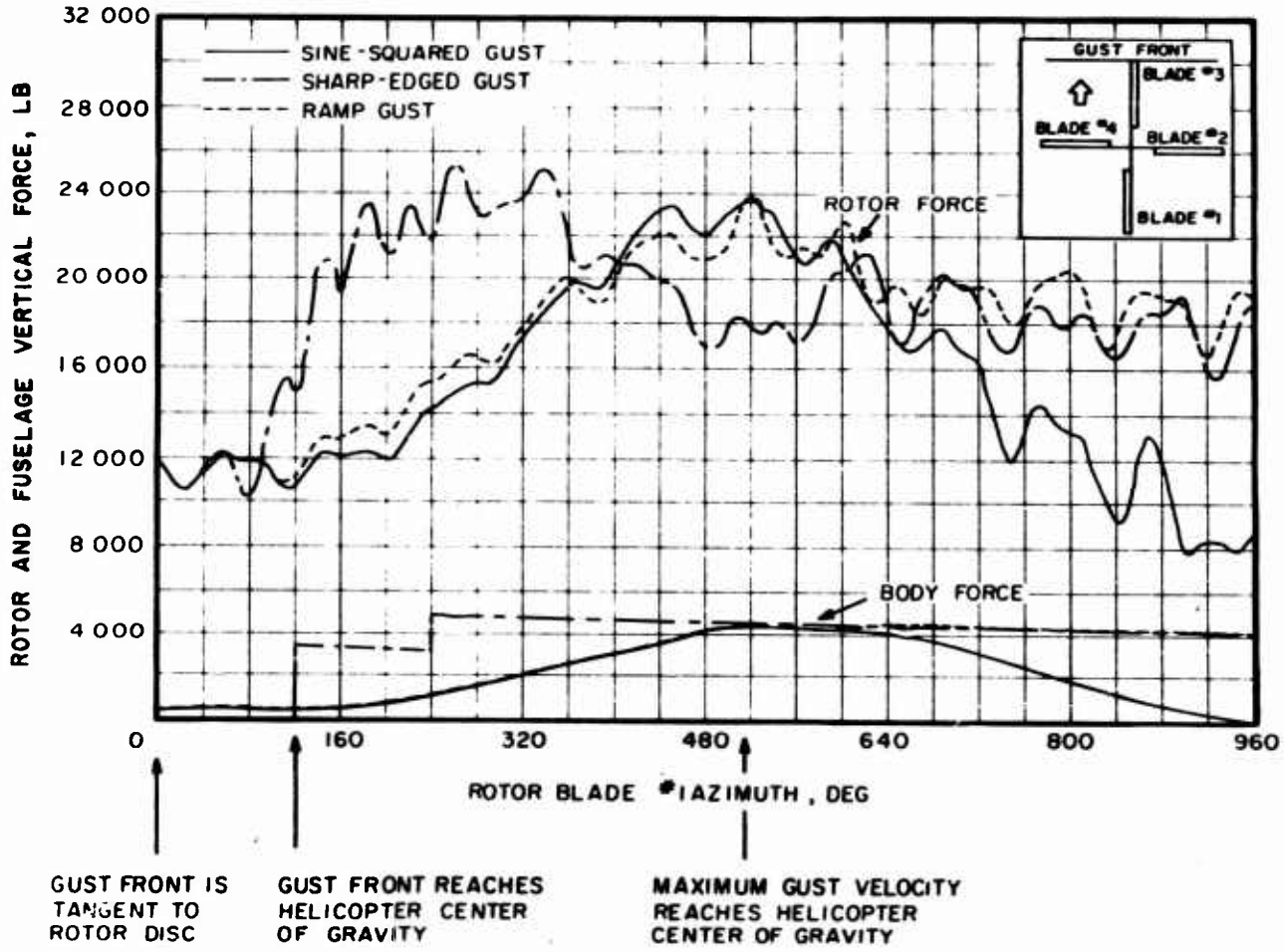

Figure 4. Azimuthal Variation of Rotor and Body Aerodynamic Vertical Force for Different Gust Shapes; $\mu = 0.5$, $\gamma = 10.0$, $C_Z/\sigma = 0.06$, Articulated Rotor.

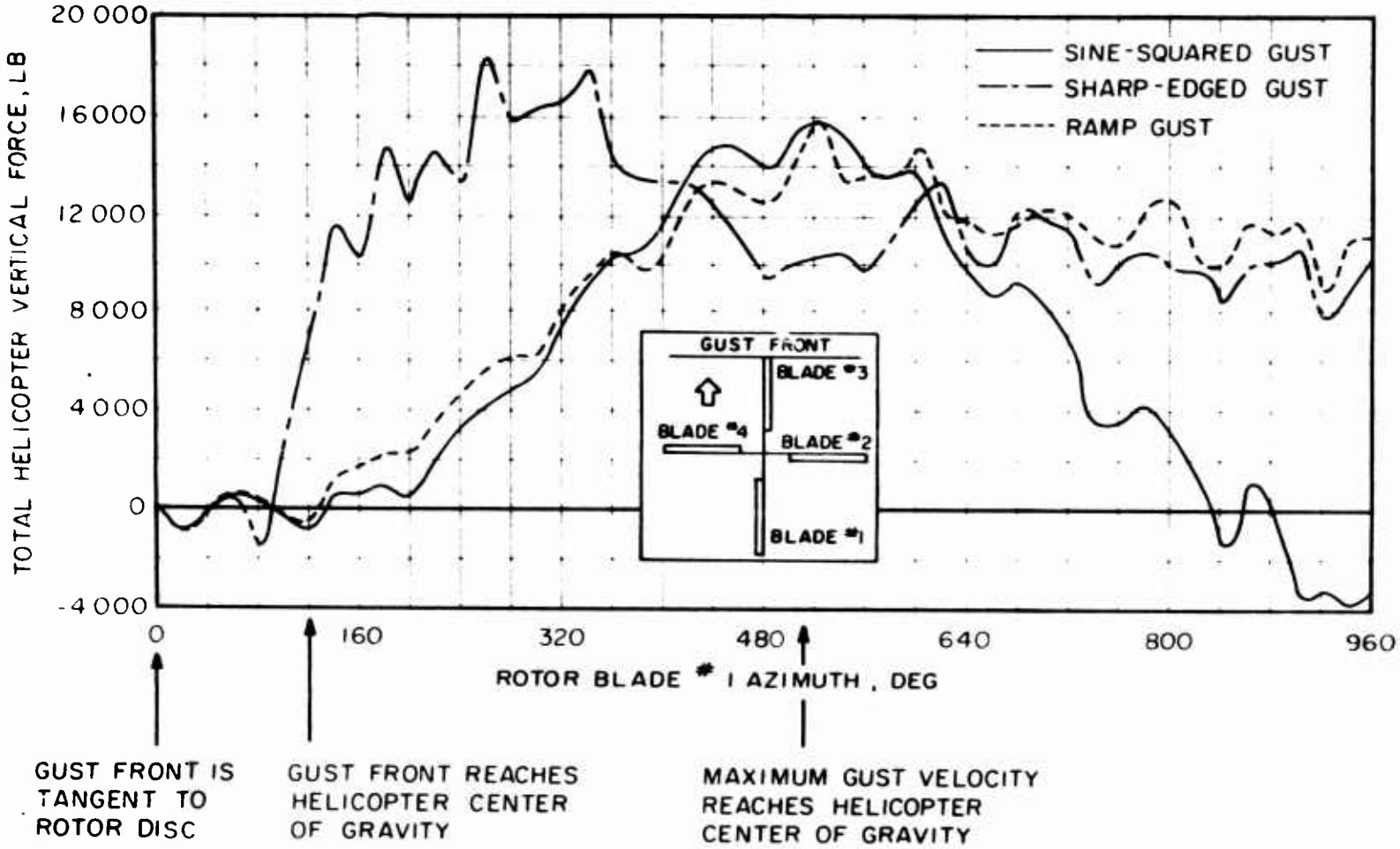

Figure 5. Azimuthal Variation of Helicopter Vertical Force for Different Gust Shapes; $\mu = 0.5$, $\gamma = 10.0$, $C_Z/\sigma = 0.06$, Articulated Rotor.

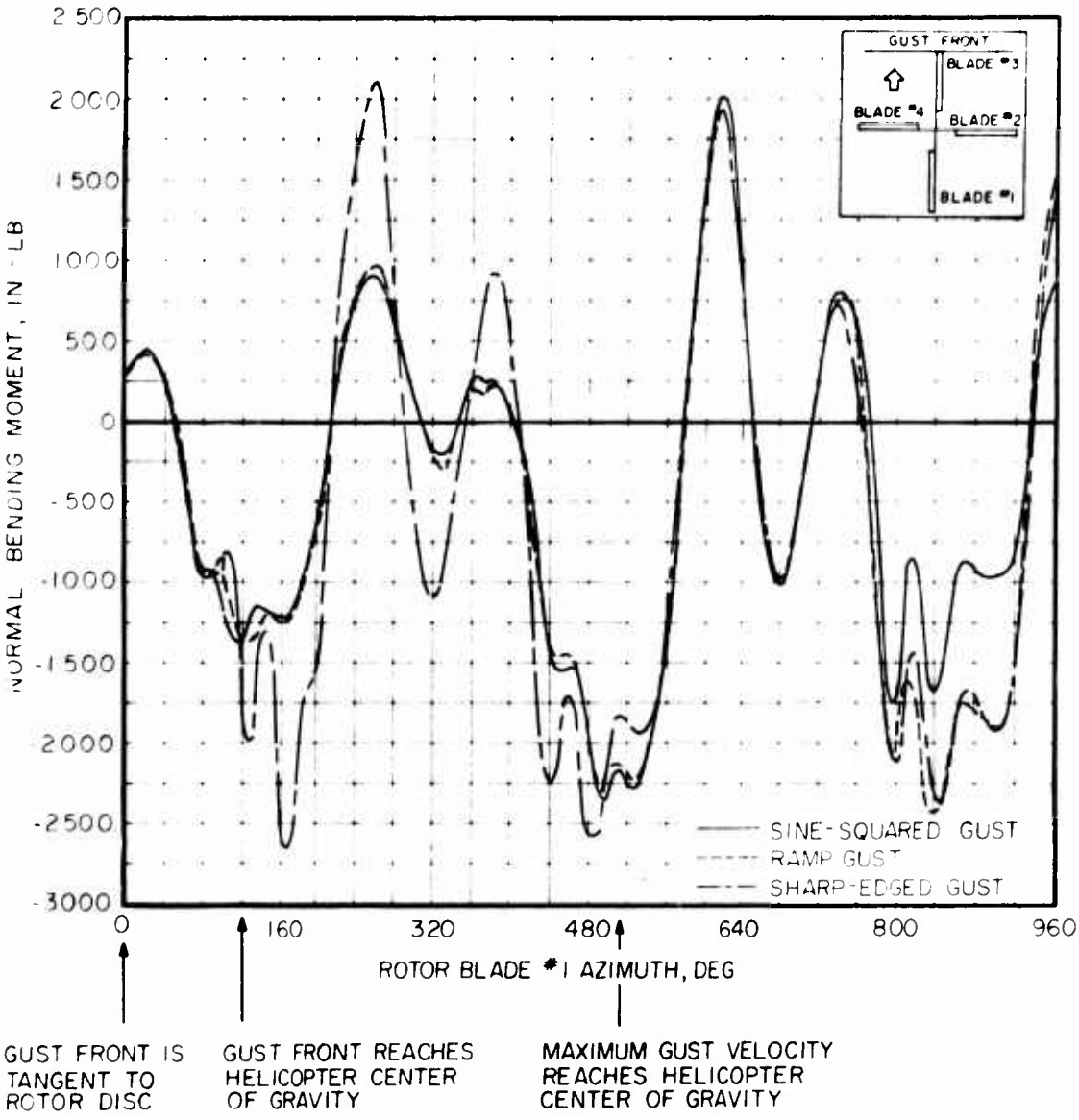

Figure 6. Azimuthal Variation of Normal Bending Moment for Different Gust Shapes; $\mu = 0.5$, $\gamma = 10.0$, $C_T/\sigma = 0.06$, Station 0.6 Radius.

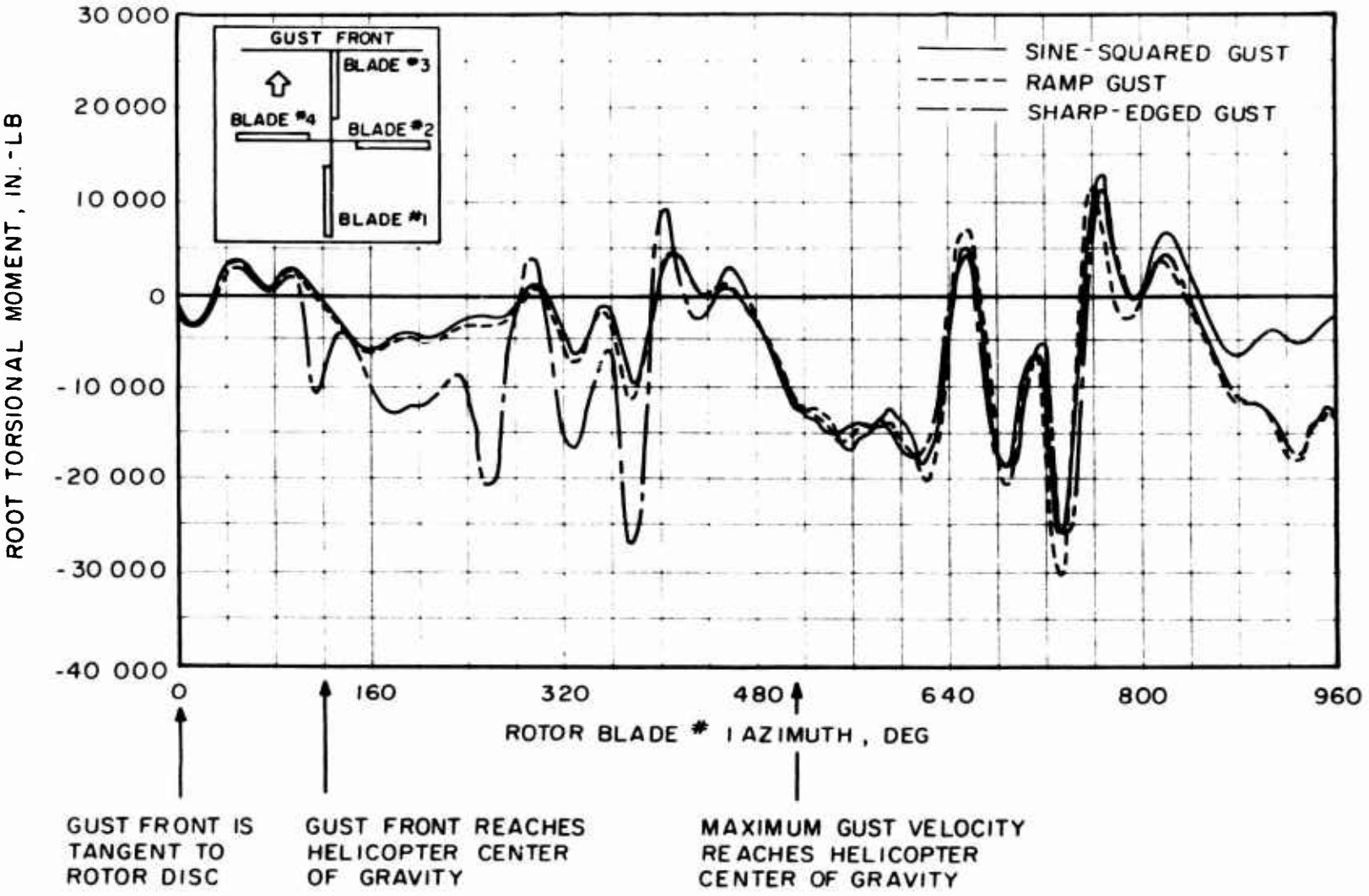

Figure 7. Azimuthal Variation of Root Torsional Moment for Different Gust Shapes; $\mu = 0.5$, $\gamma = 10.0$, $C_Z/\sigma = 0.06$, Articulated Rotor.

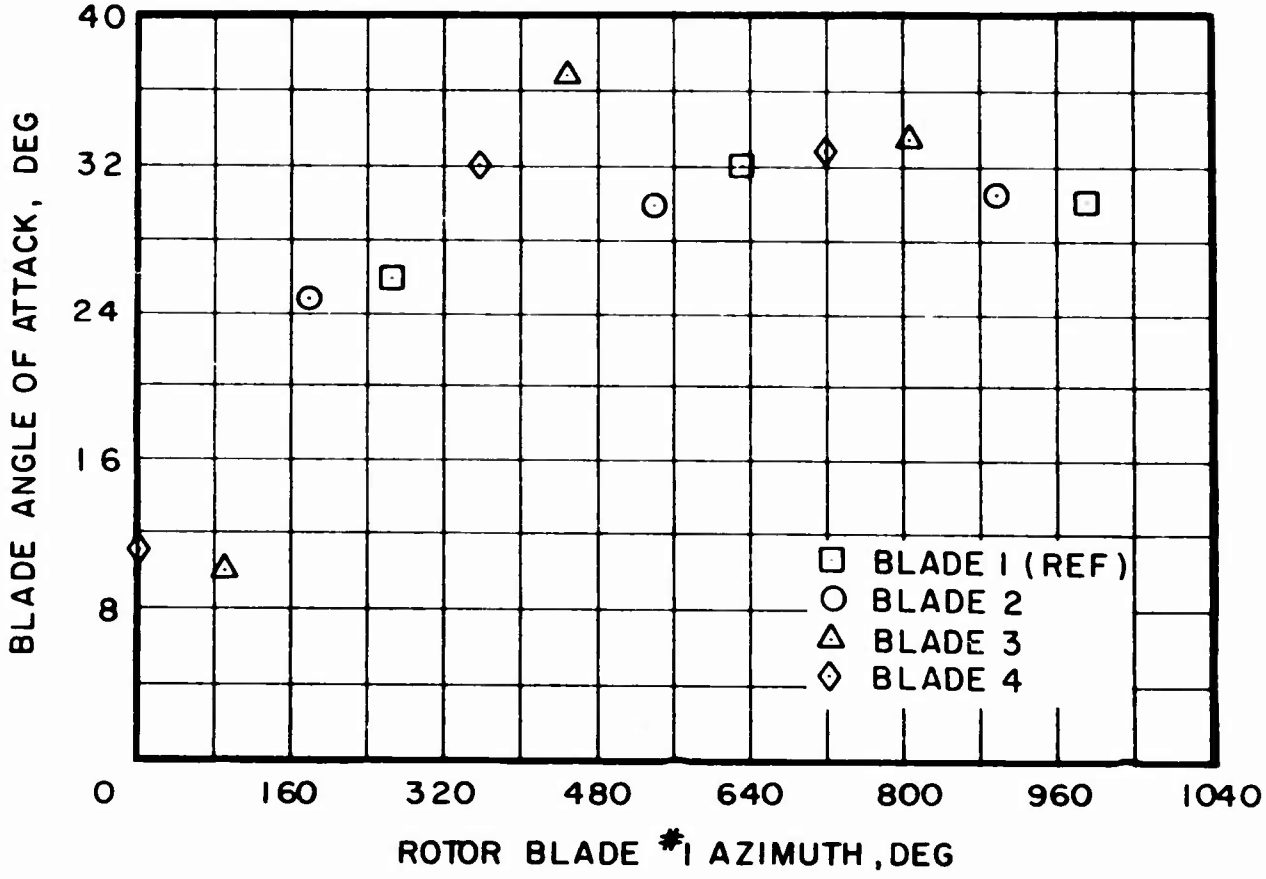

Figure 8. Angle of Attack at .75 Radius, Azimuth 270 Degrees for each Blade; $\mu = 0.5$, $\gamma = 10.0$, $C_Z/\sigma = 0.06$, Articulated Rotor, 50 ft/sec Sharp-Edged Gust.

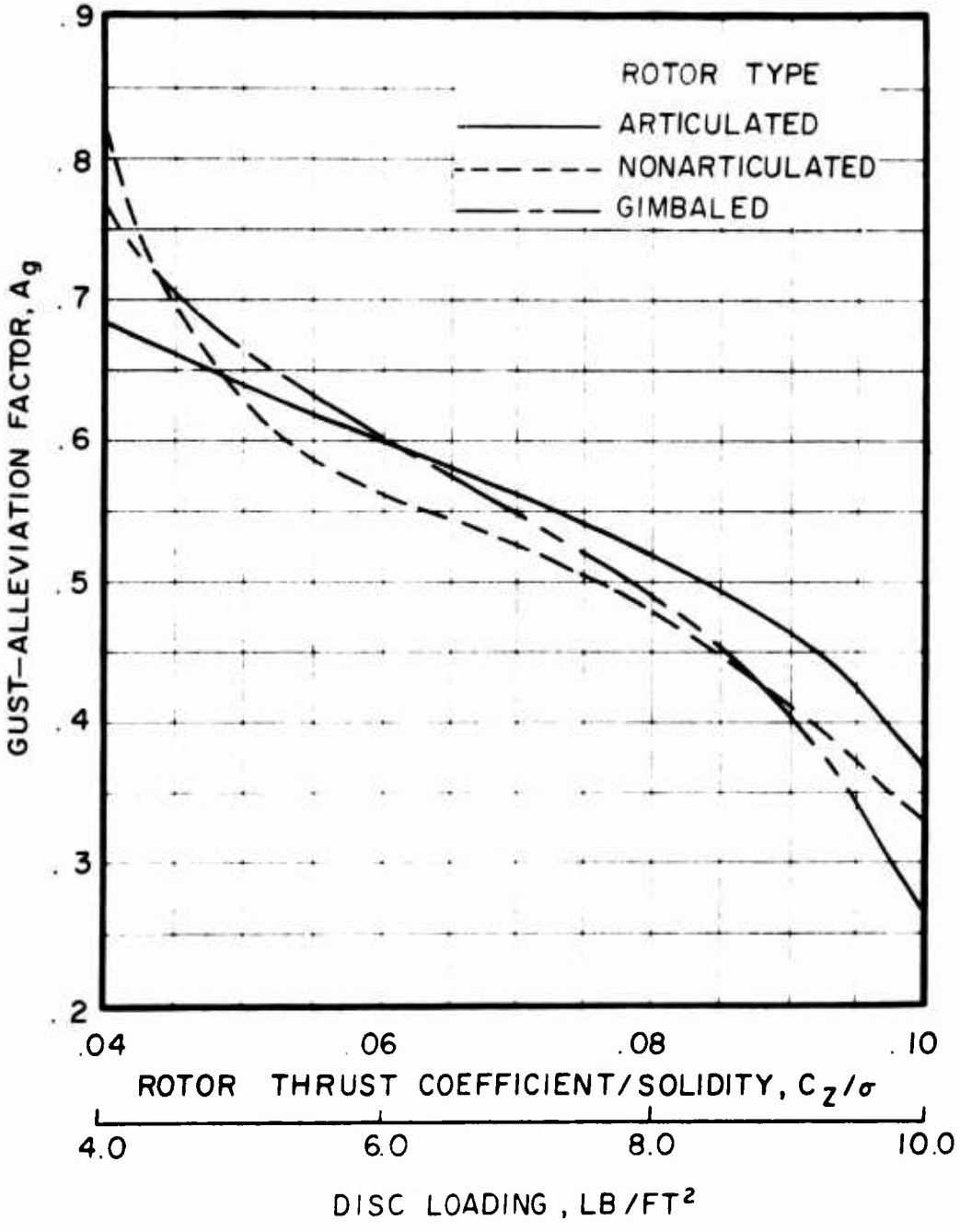

Figure 9. Effect of Rotor Loading on Gust-Alleviation Factor, $\gamma = 10$, $\sigma = 0.085$, Tip Speed = 700 ft/sec, $\rho = 0.002378$ lb-sec^2/ft^4.

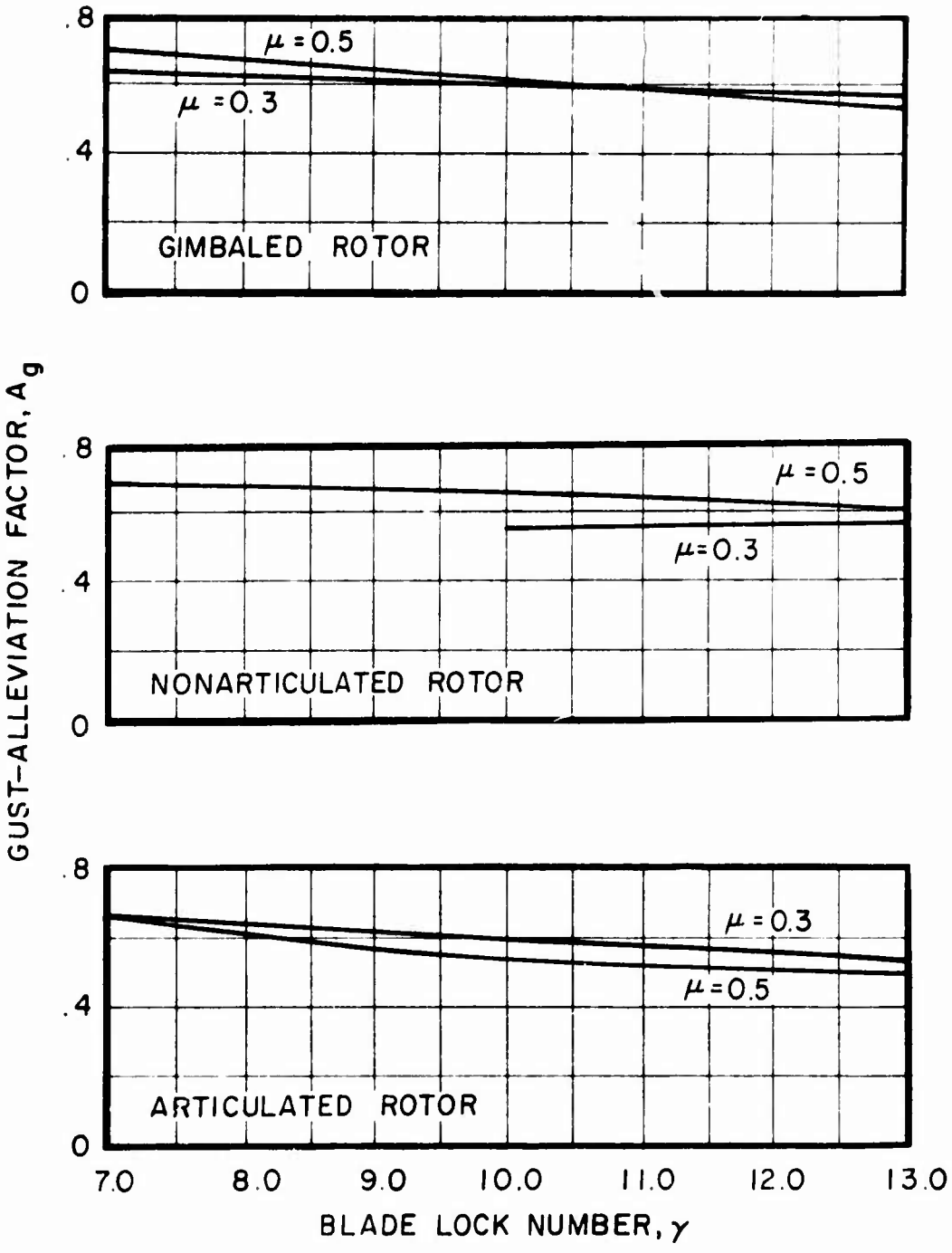

Figure 10. Effect of Lock Number and Advance Ratio on Gust-Alleviation Factor; $C_Z/\sigma = 0.06$, 50 ft/sec Sine-Squared Gust.

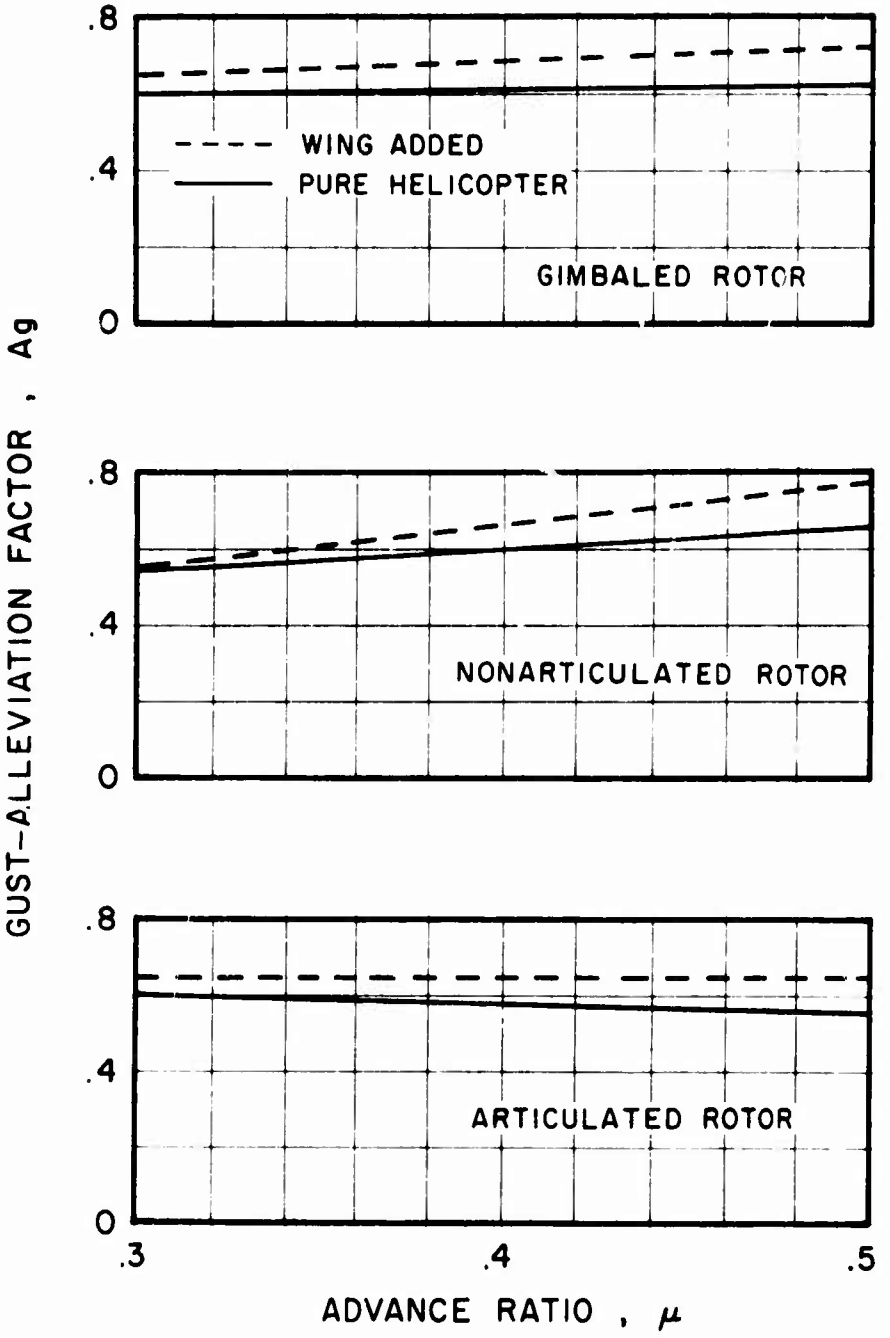

Figure 11. Effect of Compounding on Gust-Alleviation Factor; $C_Z/\sigma = 0.06$, $\gamma = 10.0$, 50 ft/sec Sine-Squared Gust.

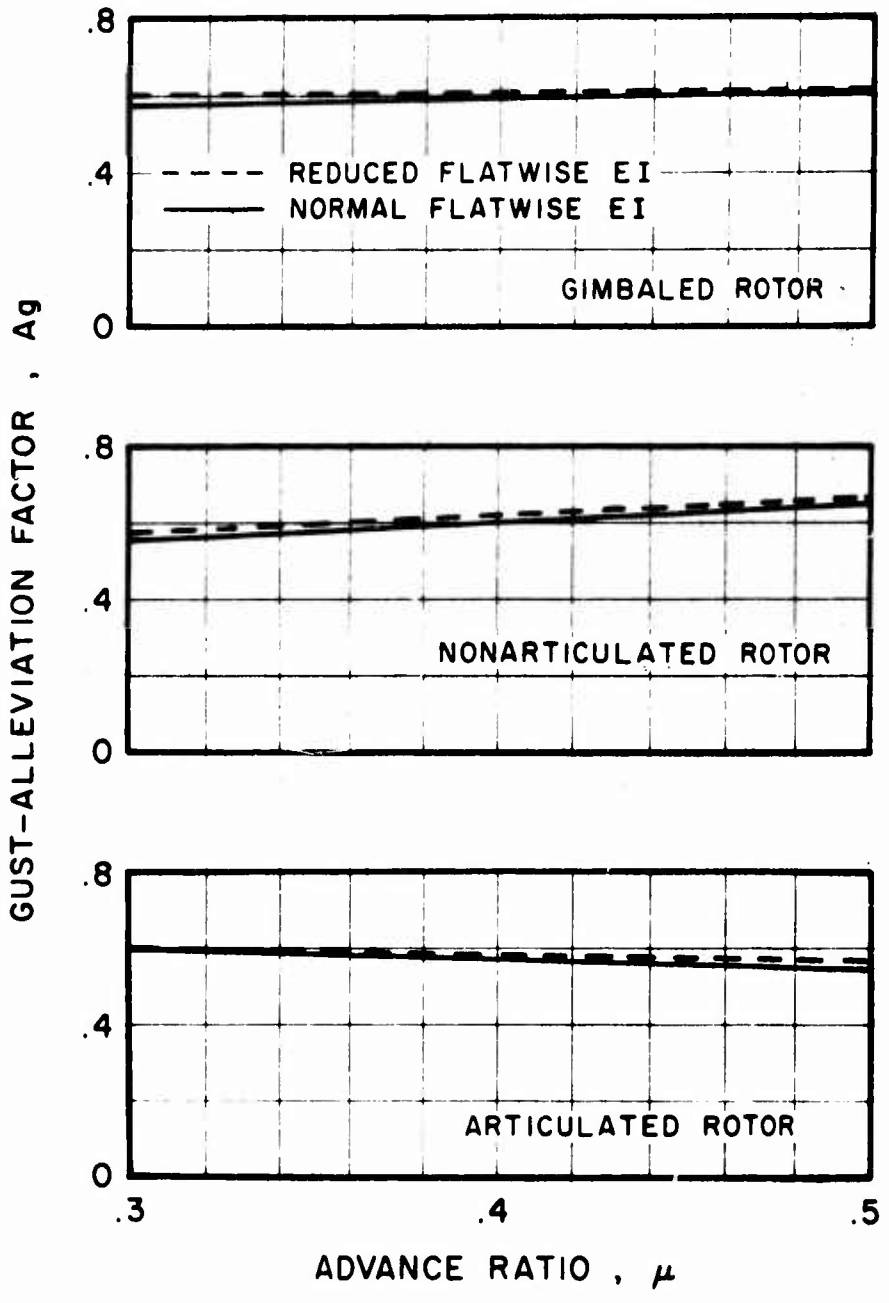

Figure 12. Effect of Reduced Flatwise Stiffness on Gust-Alleviation Factor; $C_Z/\sigma = 0.06$, $\gamma = 10.0$, 50 ft/sec Sine-Squared Gust.

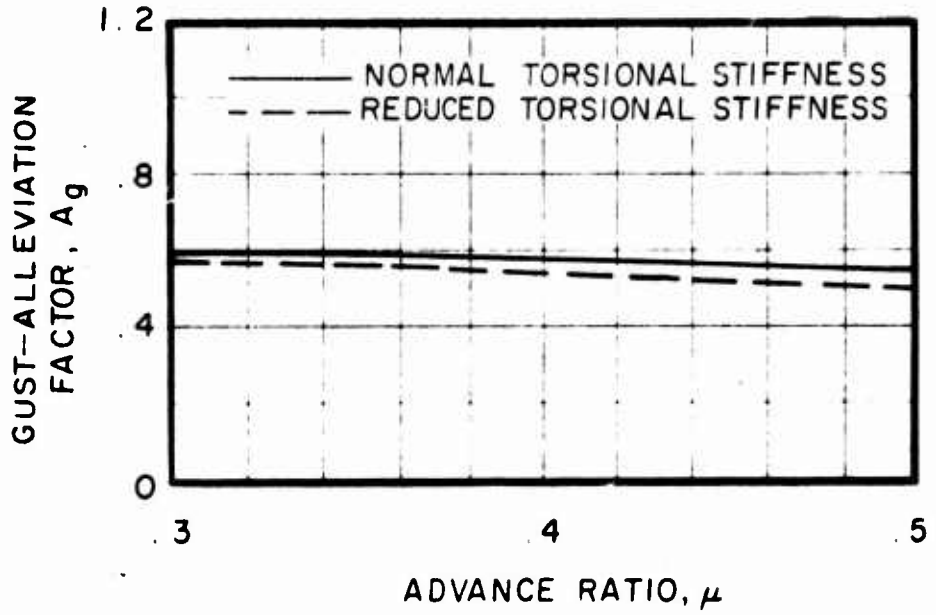

Figure 13. Effect of Reduced Torsional Stiffness on Gust-Alleviation Factor for an Articulated Rotor; $C_z/\sigma = 0.06$, $\gamma = 10.0$, 50 ft/sec Sine-Squared Gust.

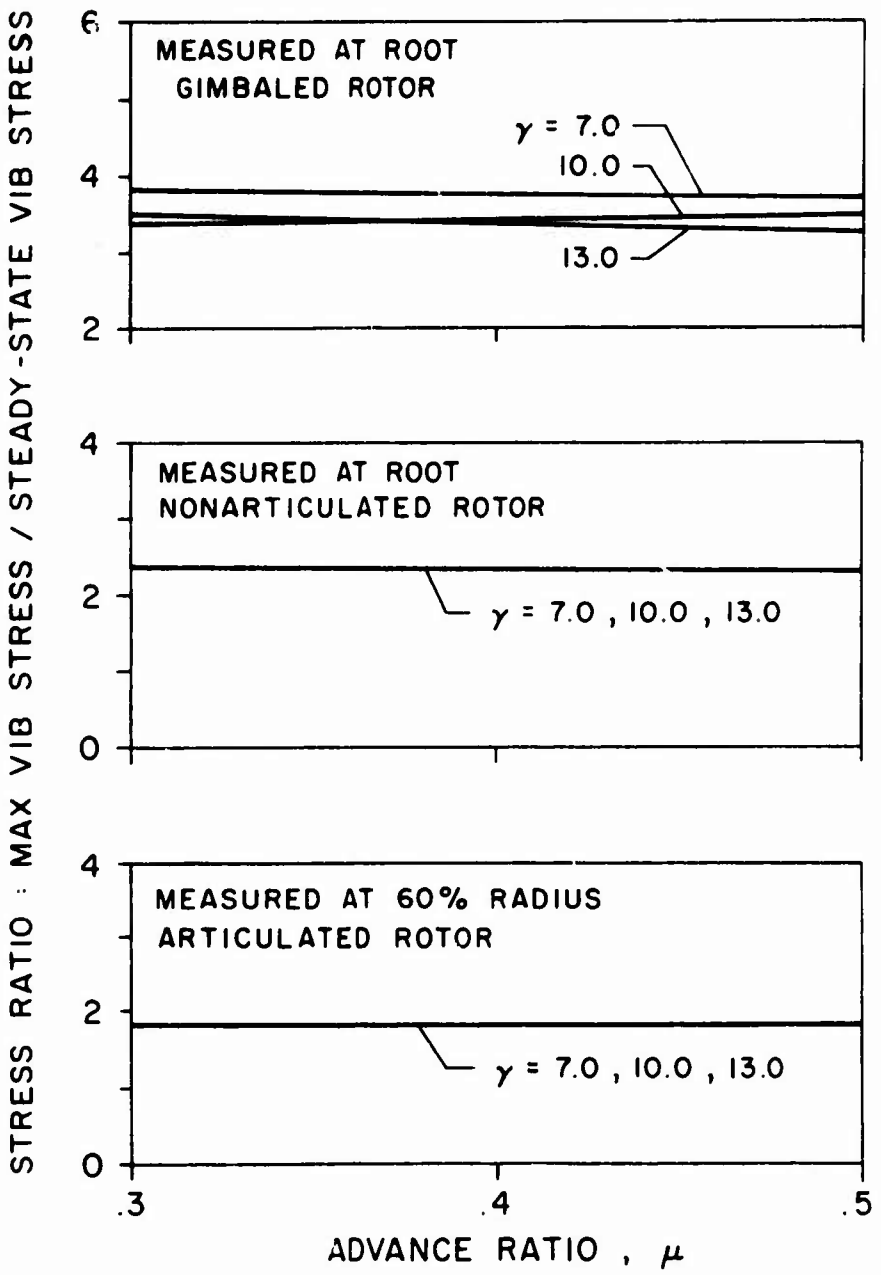

Figure 14. Effect of Advance Ratio and Lock Number on Stress Ratio; $C_Z/\sigma = 0.06$, 50 ft/sec Sine-Squared Gust.

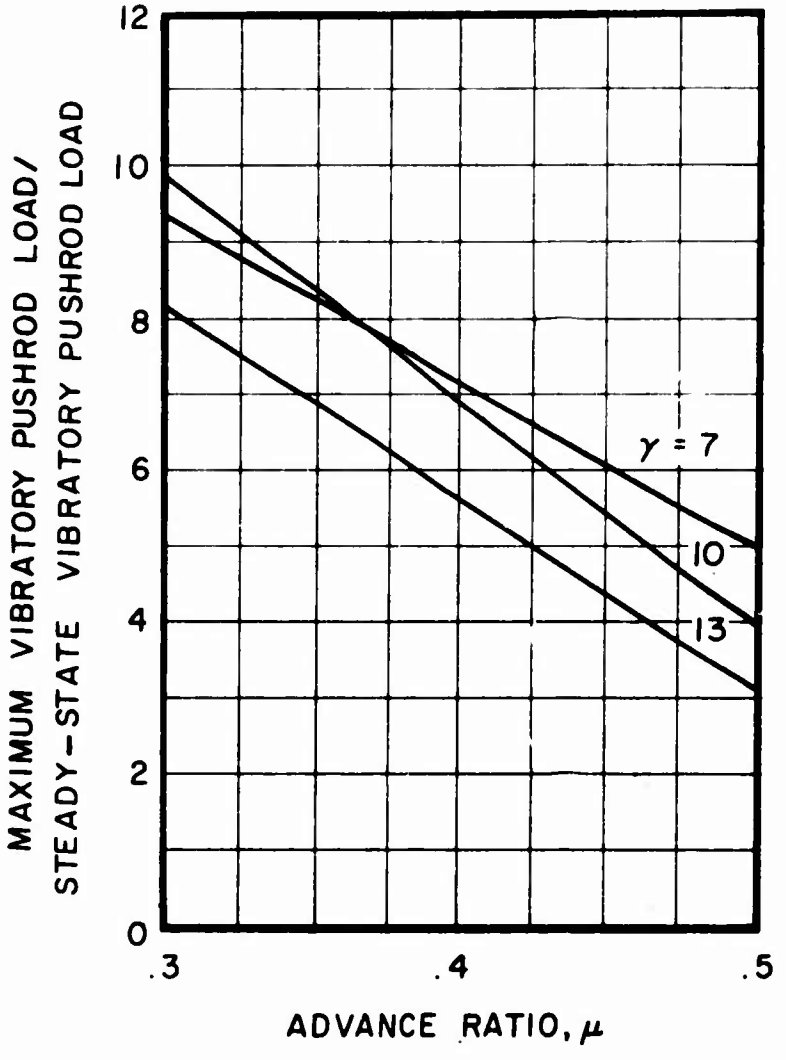

Figure 15. Effect of Advance Ratio and Lock Number on Push-rod Load Ratio; $C_Z/\sigma = 0.06$, Articulated Rotor, 50 ft/sec Sine-Squared Gust.

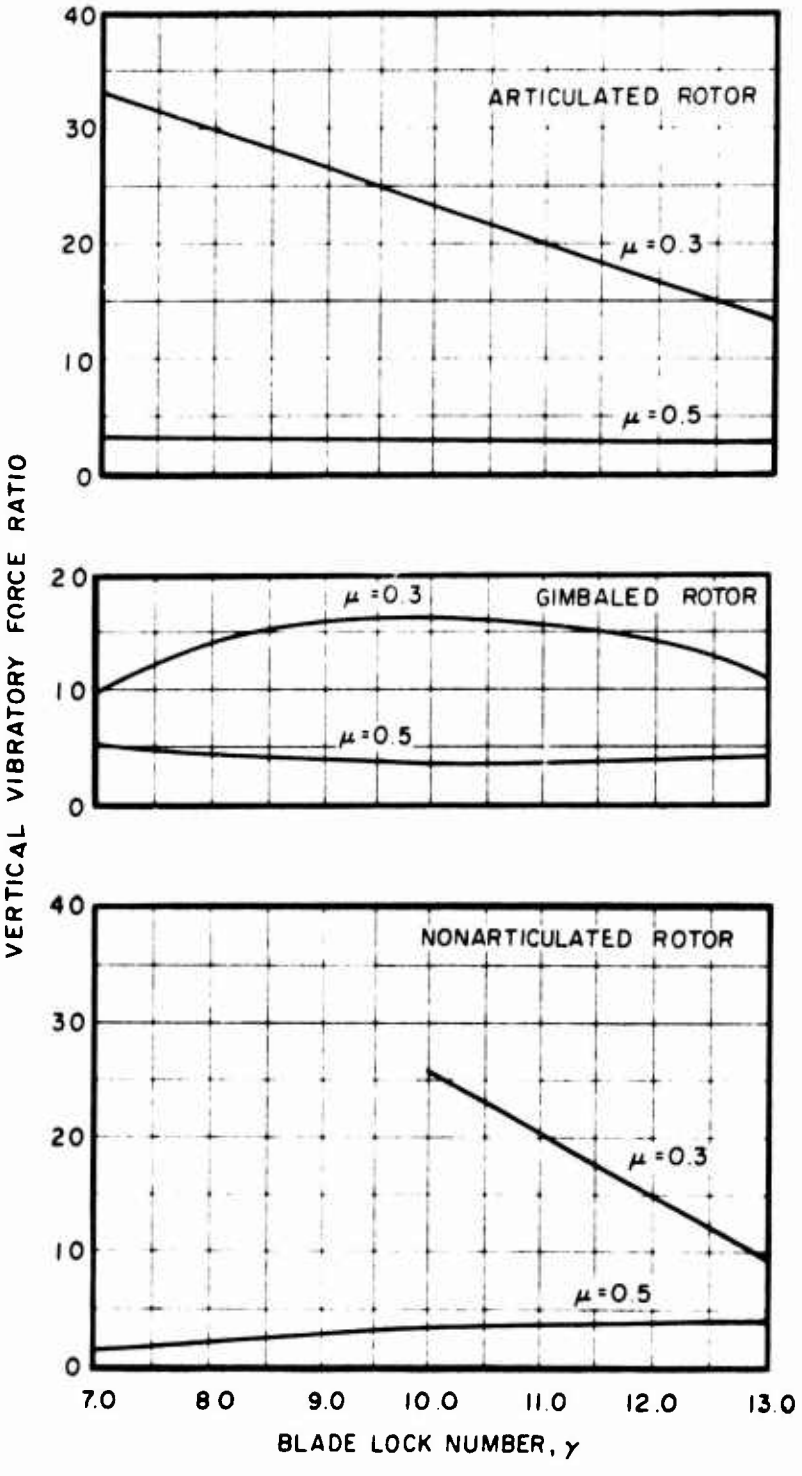

Figure 16. Effect of Lock Number on Vertical Vibratory Force Ratio; C_Z/σ = 0.06, 50 ft/sec Sine-Squared Gust.

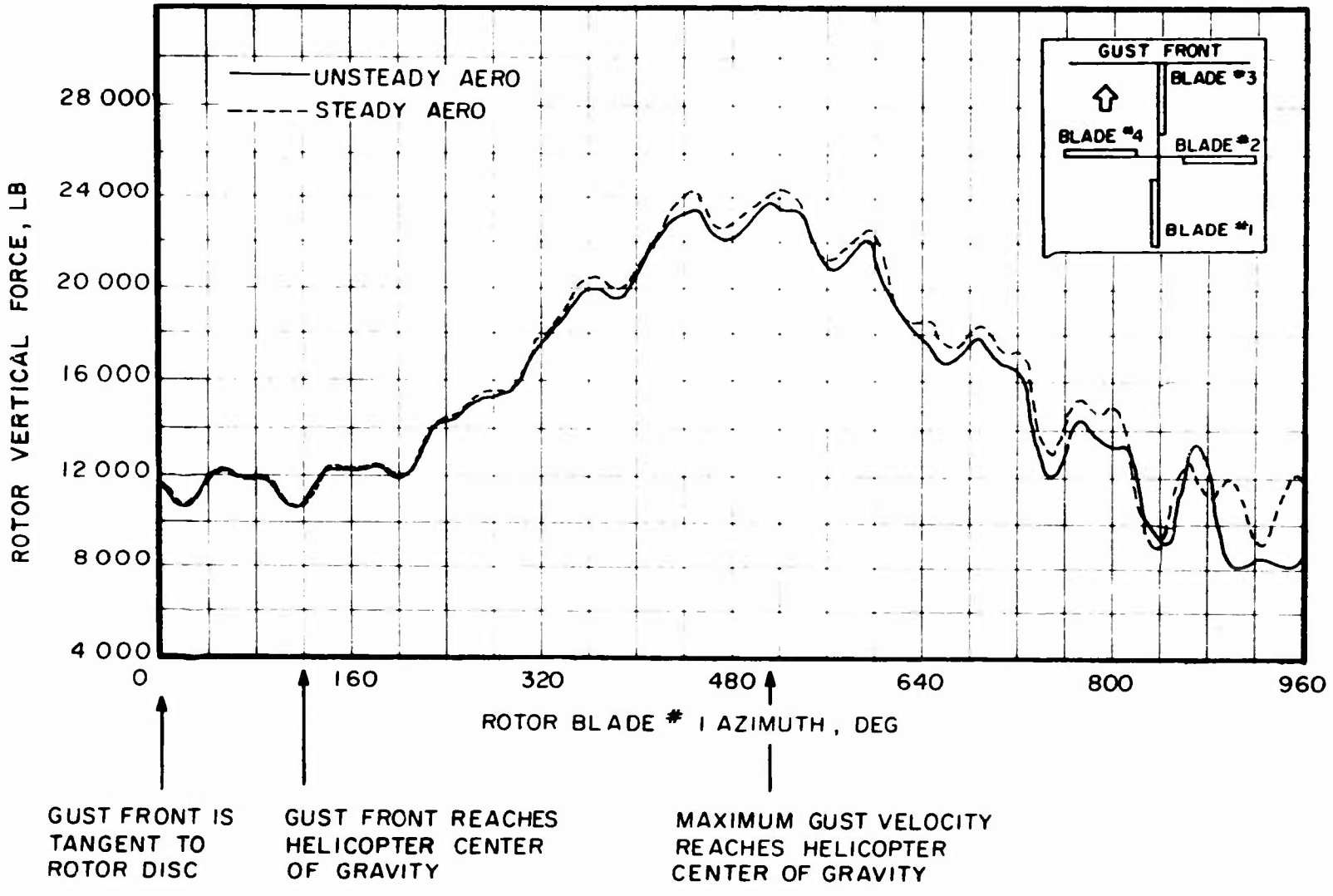

Figure 17. Effect of Fuselage Motion on Rotor Vertical Force for an Articulated Rotor; Sine-Squared Gust, $\mu = 0.5$, $\gamma = 10.0$, $C_Z/\sigma = 0.06$.

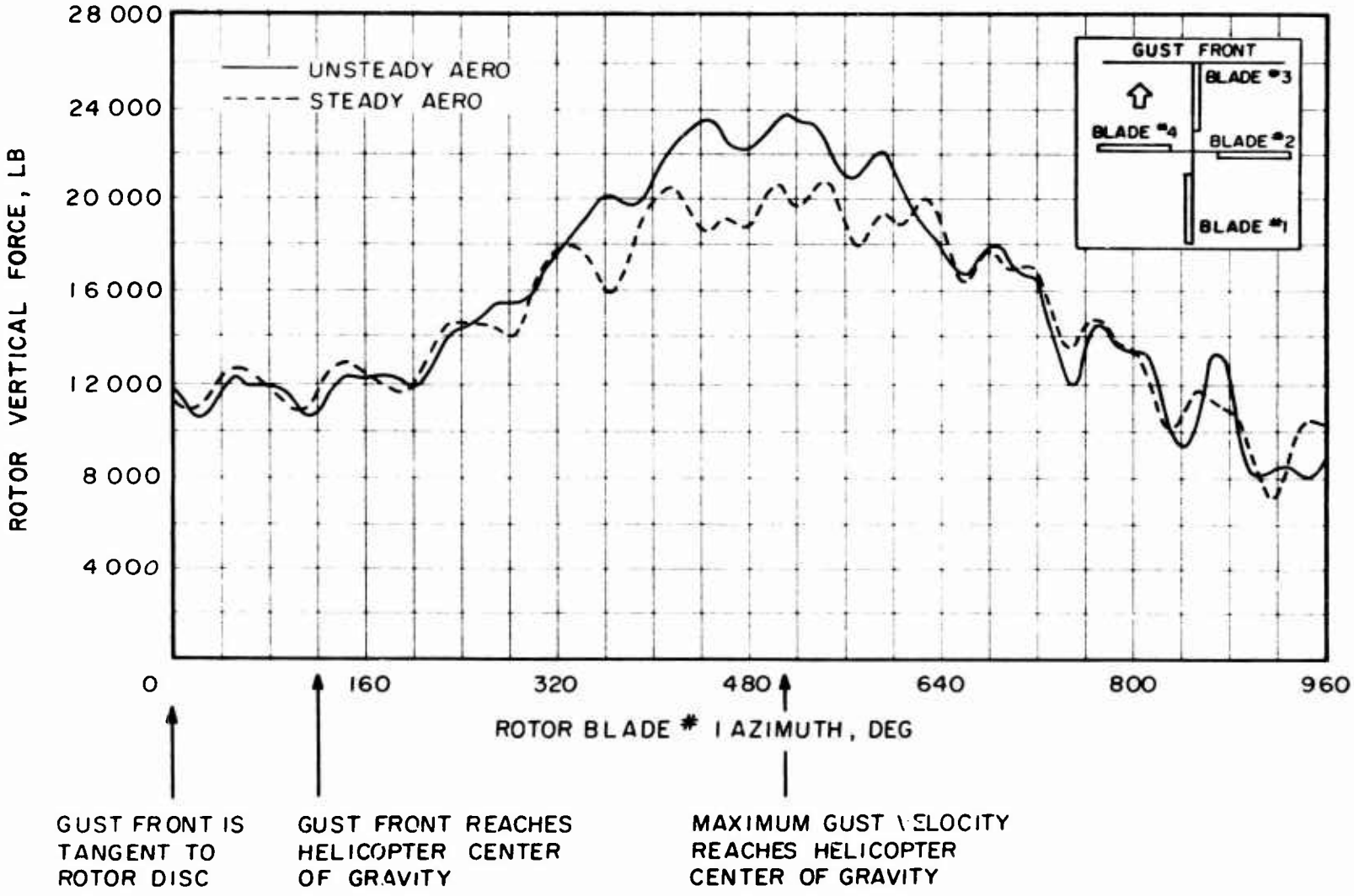

Figure 18. Effect of Unsteady Aerodynamics on Rotor Vertical Force for an Articulated Rotor; Sine-Squared Gust, $\mu = 0.5$, $\gamma = 10.0$, $C_Z/\sigma = 0.06$.

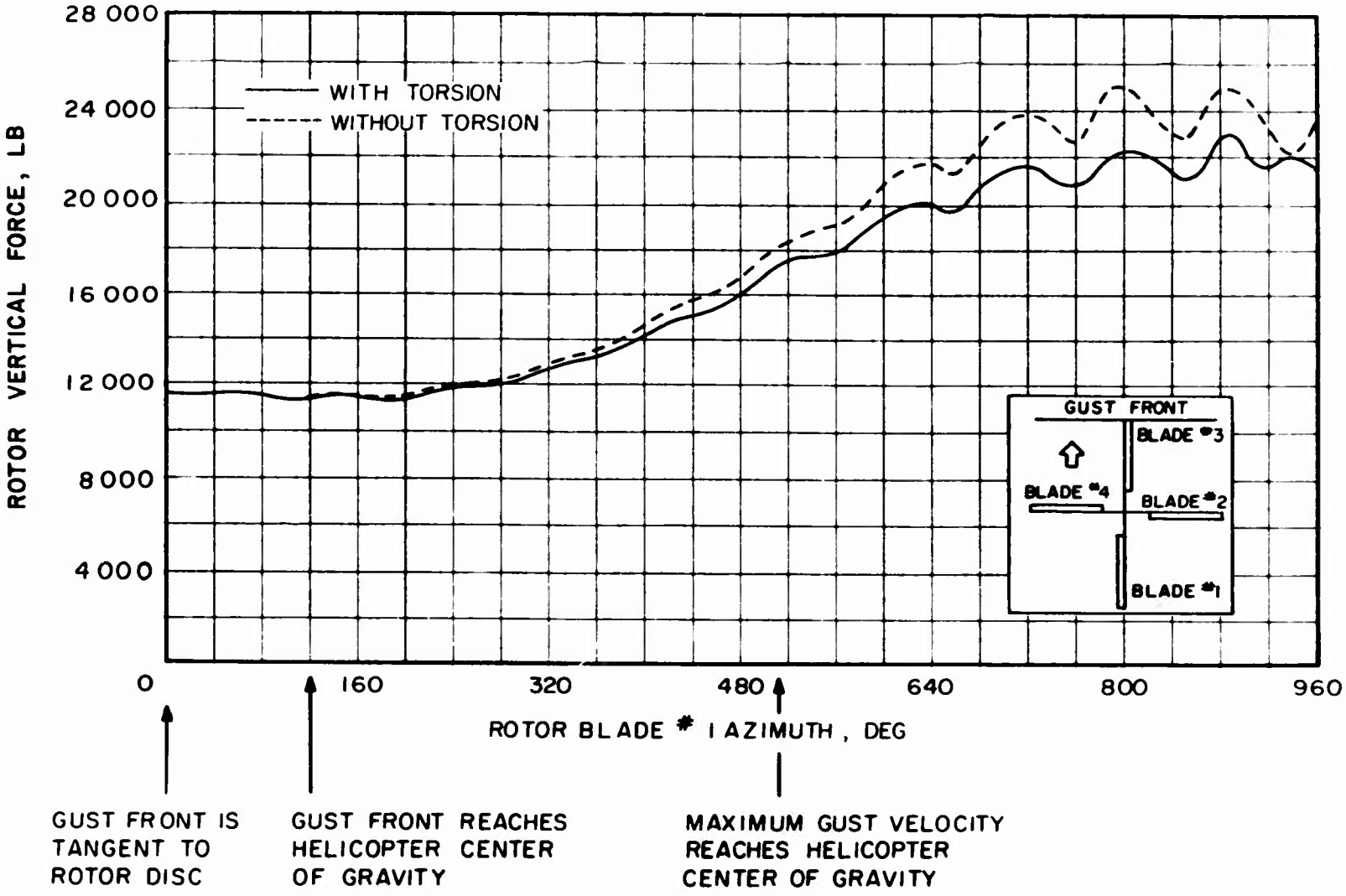

Figure 19. **Effect of Torsional Degree of Freedom on Rotor Vertical Force for an Articulated Rotor; Sine-Squared Gust,** $\mu = 0.5$, $\gamma = 10.0$, $C_Z/\sigma = 0.06$.

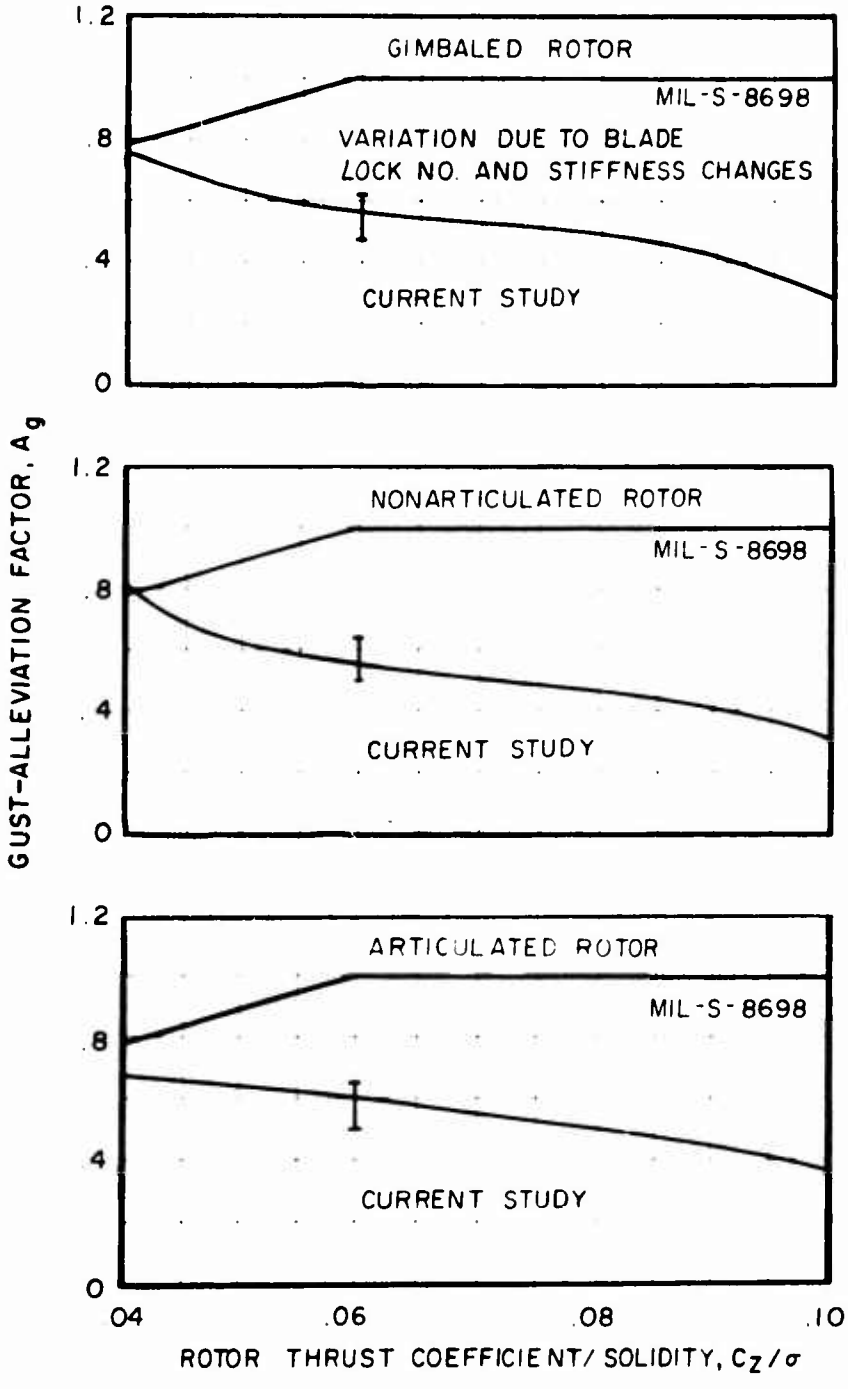

Figure 21. Summary Plot of Gust-Alleviation Factor; σ = 0.085, Tip Speed = 700 ft/sec, ρ = 0.002378 lb-sec^2/ft^4.

LITERATURE CITED

1. Crim, Almer D., GUST EXPERIENCE OF A HELICOPTER AND AN AIRPLANE IN FORMATION FLIGHT, NACA Technical Note 3354, NACA, 1954.

2. Harvey, K. W., Blankenship, B. L., and Drees, J. M., ANALYTICAL STUDY OF HELICOPTER GUST RESPONSE AT HIGH FORWARD SPEEDS, Bell Helicopter Company; USAAVLABS Technical Report 69-1, U. S. Army Aviation Materiel Laboratories, Fort Eustis, Virginia, September 1969, AD 862594.

3. Bergquist, R. R., and Thomas, G. C., TECHNICAL MANUAL FOR NORMAL MODES AEROELASTIC COMPUTER PROGRAM, July 1972.

4. Bergquist, R. R., and Thomas G. C., USER'S MANUAL FOR NORMAL MODE BLADE AEROELASTIC COMPUTER PROGRAM, July 1972.

5. Arcidiacono, P. J., PREDICTION OF ROTOR INSTABILITY AT HIGH FORWARD SPEEDS, VOLUME 1 - STEADY FLIGHT DIFFERENTIAL EQUATIONS OF MOTION FOR A FLEXIBLE HELICOPTER BLADE WITH CHORDWISE MASS UNBALANCE, Sikorsky Aircraft Div., United Aircraft Corp.; USAAVLABS Technical Report 68-18A, U. S. Army Aviation Materiel Laboratories, Fort Eustis, Virginia, February 1969, AD 685860.

6. Arcidiacono, P. J., Carta, F. O., Cassellini,L. M., and Elman,H. L., INVESTIGATION OF HELICOPTER CONTROL LOADS INDUCED BY STALL FLUTTER, Sikorsky Aircraft Div., United Aircraft Corp., USAAVLABS Technical Report 70-2, March 1970, AD 869823.

7. Landgrebe, Anton J., AN ANALYTICAL METHOD FOR PREDICTING ROTOR WAKE GEOMETRY, United Aircraft Research Laboratories; Journal of the American Helicopter Society, Vol. 14, No. 4, October 1969, pp. 20-32.

8. Bailey, F. J., Jr., A SIMPLIFIED THEORETICAL METHOD OF DETERMINING THE CHARACTERISTICS OF A LIFTING ROTOR IN FORWARD FLIGHT, NACA Report No. 716.

9. Landgrebe, A. J., SIMPLIFIED PROCEDURES FOR ESTIMATING FLAPWISE BENDING MOMENTS ON HELICOPTER ROTOR BLADES, NASA CR-1440, October 1969.

10. Bellinger, E. D., ANALYTICAL INVESTIGATION OF THE EFFECTS OF UNSTEADY AERODYNAMICS, VARIABLE INFLOW AND BLADE FLEXIBILITY ON HELICOPTER ROTOR STALL CHARACTERISTICS. NASA CR-1769.